The published version can be found at: https://doi.org/10.1016/j.marenvres.2022.105584

# Benthos response to nutrient enrichment and functional consequences in coastal ecosystems

Ludovic Pascal[1,*], Gwénaëlle Chaillou[1], Christian Nozais[2], Joannie Cool[1], Pascal Bernatchez[3], Kevin Letourneux[1], Philippe Archambault[4]

[1] Institut des sciences de la mer de Rimouski, Québec-Océan, Canada Research Chair in geochemistry of coastal hydrogeosystems, Université du Québec à Rimouski, 310 Allée des Ursulines, Rimouski, Québec G5L 3A1, Canada

[2] Département de biologie, chimie et géographie, Québec-Océan, Université du Québec à Rimouski, 300 Allée des Ursulines, Rimouski, QC, G5L 3A1, Canada

[3] Research Chair in Coastal Geoscience, Québec-Océan, Département de biologie, chimie et géographie, Université du Québec à Rimouski, 300 Allée des Ursulines, Rimouski, QC, G5L 3A1, Canada

[4] ArcticNet, Québec-Océan, Département de biologie, Université Laval, 2325 rue de l'Université, Québec, QC, G1V 0A6, Canada

[*] Corresponding author: Ludovic Pascal (ludovic_pascal@uqar.ca)

The published version can be found at: https://doi.org/10.1016/j.marenvres.2022.105584

## Highlights

- Ex-situ experiment studying effects of fertilisation on benthic compartment
- Fertilisation increased organic matter content at the sediment surface
- Fertilisation increased the concentration of reduced chemical species in porewater
- Fertilisation reduced the penetration depth of macroinfauna
- In enriched treatments, sediment became a source of nutrients for the water column

## Graphical abstract

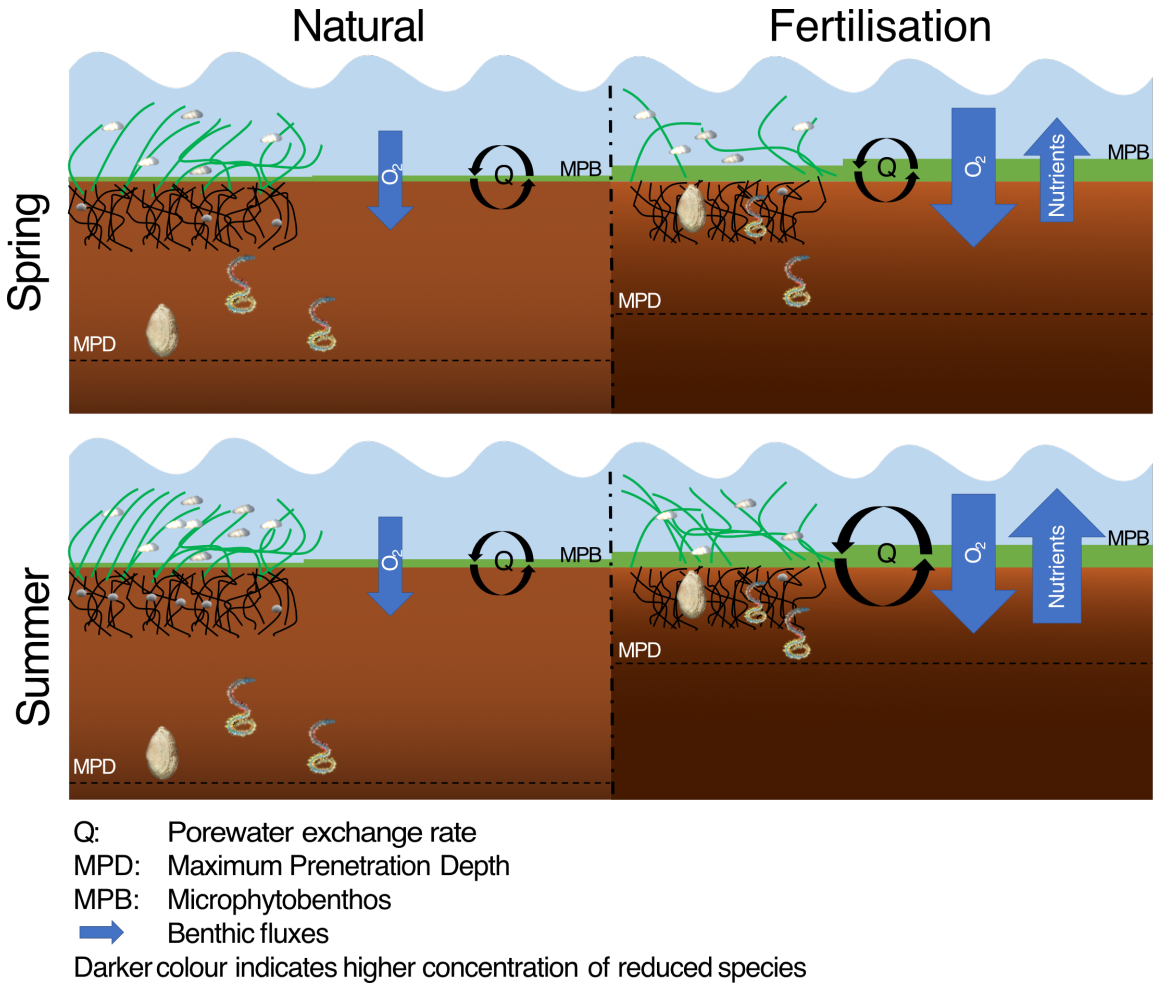

The published version can be found at: https://doi.org/10.1016/j.marenvres.2022.105584

**Abstract**

As land use intensifies, many coastal waters are becoming enriched with otherwise limiting nutrients, leading to eutrophication. While the extreme effects of eutrophication on benthic communities are well documented, there is still a lack of knowledge about how nutrient enrichment alters biogeochemical interactions occurring at the sediment-water interface. Using *ex-situ* experiments, this study explores the consequences of nutrient enrichment on sediment characteristics, macrofauna community and benthic fluxes. The quantity of sedimentary organic matter and porewater concentration of $NH_4^+$, $NO_x$ and $PO_4^{3-}$ increased in enriched treatments. These changes did not affect the macrobenthic community structure. However, macroinfauna buried less deep and increased their ventilation activity. As consequences, nutrient efflux increased, thereby favouring eutrophication processes. These effects were reduced in presence of seagrass, thus illustrating the buffering capacity of seagrass in the context of environmental changes, and particularly, of eutrophication. Overall, this study highlights that the functional consequences of nutrient enrichment involve interconnected processes that are variable in space and time.

*Keywords:* Eutrophication, Seagrass, Macrofauna, Biogeochemistry, Bioturbation, Benthic-pelagic coupling, Fertilizers, Ecosystem functioning, Oxygen, Nutrient

The published version can be found at: https://doi.org/10.1016/j.marenvres.2022.105584

## 1 Introduction

Along the land-ocean continuum, coastal ecosystems received and exchange substantial amounts of organic matter (OM) and nutrients from/with terrestrial and oceanic ecosystems. They harbour diversified habitats (Barbier et al., 2011) and account for up to a third of the oceanic primary production and about 90 % of the sedimentary mineralization of OM (Borges, 2005; Gattuso et al., 1998; Wollast, 1998). Hence, despite their low surface areas (7 % of the oceanic surface area), coastal ecosystems are among the most productive ecosystems in the world (Gattuso et al., 1998). The exchange of particles and nutrients between the sediment and the water column, so-called benthic-pelagic coupling, is of paramount importance in the functioning of these shallow ecosystems (Chauvaud et al., 2000; Hochard et al., 2019). One of the most crucial factors controlling benthic-pelagic coupling is the composition of benthic communities. For instance, macrophytes, such as seagrasses, are known to influence benthic biogeochemistry. Seagrasses are a sink for nutrients, which they assimilate from both the water column and the sediment (Touchette and Burkholder, 2000). Their leaves reduce local hydrodynamics, enhancing sedimentation of fine organic-rich particles (Hemminga and Duarte, 2000). Benthic macrofauna also play a critical role in benthic-pelagic coupling through their influence on OM mineralization and nutrient cycling at the sediment-water interface (Link et al., 2013; Snelgrove et al., 2018). In addition to their direct effect on OM mineralization (*i.e.*, OM consumption and their metabolism; Middelburg, 2019), benthic macrofauna influence OM mineralization through bioturbation (*sensu* Kristensen et al., 2012). By mixing sediment particles, benthic macrofauna transfer freshly deposited particulate OM deeper in the sediment column where oxygen is absent or, the other way around, transport buried refractory particulate OM to

oxygenated layers of the sediment column (Kristensen et al., 2012). By ventilating their burrows, benthic macrofauna promote the transport of oxygen into otherwise anoxic sediment layers (Volkenborn et al., 2016). Overall, these bioturbation processes increase OM mineralization and nutrient efflux from the sediment (Aller and Aller, 1998), thus enhancing ecosystem function such as primary production (Lohrer et al., 2004).

With more than a third of the human population living in coastal regions (Boström et al., 2011), coastal ecosystems are also exposed to anthropogenic disturbances. Intense land use and wastewater production result in substantial inputs of nitrogen (N) and phosphorus (P) nutrients in coastal waters leading to eutrophication and subsequent oxygen depletion in many ecosystems (Nixon, 1998; Rabalais et al., 2009). While relatively low nutrient enrichment has been shown to promote the seagrass community's growth (Alcoverro et al., 1997; Brun et al., 2002), eutrophication appears to be one of the most probable causes of the worldwide alteration of seagrass ecosystems (Burkholder et al., 2007; Dunic et al., 2021; Orth et al., 2006; Waycott et al., 2009). High nutrient concentrations in the water column stimulate primary production, reducing the light penetration and its availability for seagrass (Lapointe et al., 2020; Lee et al., 2007). High nutrient concentrations can also affect seagrass and associated macrobenthic community survival through direct ammonium toxicity, changes in OM quantity and quality and reduced oxygen concentration and sediment biogeochemistry (Brodersen et al., 2017; Burkholder et al., 1992; Moreno-Marín et al., 2016; Pearson and Rosenberg, 1978; Riedel et al., 2016). Therefore, the effects of nutrient enrichment on macrobenthic communities involve complex interconnected mechanisms that need to be teased apart to fully understand the functional consequences of nutrient enrichment. Although the overall and

The published version can be found at: https://doi.org/10.1016/j.marenvres.2022.105584

extreme effects of eutrophication on macrobenthic communities are well-known (*e.g.*, Grall and Chauvaud, 2002), there is still a lack of information concerning how benthic processes feedbacks to nutrient enrichment can mitigate or favour eutrophication.

This study aimed at assessing the mechanisms involved in the benthic response to nutrient enrichment in coastal ecosystems. More specifically, it is anticipated that nutrient enrichment in the water column increases OM quantity and quality at the sediment surface, resulting in higher porewater concentrations of nutrients and lower oxygen penetration depth. Such changes in sediment biogeochemistry are expected to reduce the abundance of non-tolerant species and the foraging activity of more-tolerant ones resulting in lower bioturbation rates and thus altering benthic fluxes at the sediment water interface. Finally, it is expected that the presence of seagrass, through nutrient assimilation, buffers the effects of nutrient enrichment. These hypotheses were addressed by two seasonal well-controlled experiments to integrate the temporal heterogeneity of coastal ecosystems.

## 2 Materials and methods

### 2.1 Study site

Sediment cores were collected in Isle-Verte Bay (48° 2' 36.76" N; 69° 21' 3.736" W, St. Lawrence estuary, QC, Canada; Figure 1A). The Isle-Verte Bay receives freshwater inputs from its eastern and southern parts and mostly by the Isle-Verte river, whose watershed (512 $km^2$) is characterized by agricultural activities (about 30 % of the watershed; OBAKIR). This bay is characterized by a semi-diurnal tide with an amplitude between 1.5 and 4.7 m, and a saltmarsh partially covers its intertidal area with cordgrass *Spartina alterniflora* in the high foreshore and a continuous *Zostera marina* meadow located between 1 and 5 m depth (with respect to the WGS-84 ellipsoid) in the

low foreshore (-2 m at the sampling site; Figure 1). This seagrass meadow is usually covered by sea ice during winter which creates long lasting ice-made tidal pools within it (see Pascal et al., 2020 for details on ice-made tidal pools). This natural patchiness in seagrass cover was used to collect samples from immediately proximate vegetated and unvegetated areas. The sediment at the sampling site consisted of muddy sand with an average grain size ($D_{50}$) and porosity of 124.2 ± 1.9 µm and 0.9 ± 0.0, respectively.

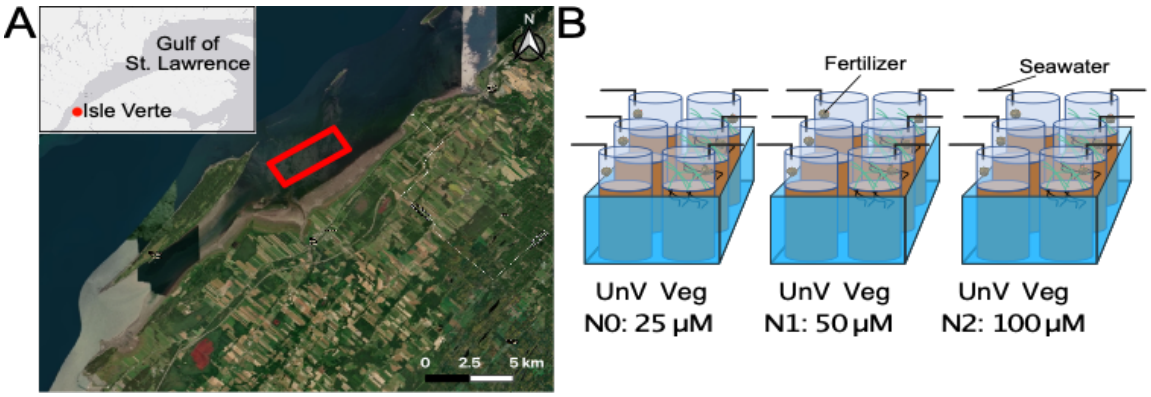


Figure 1: *Study site*. Location of Isle-Verte Bay (red point) and sampling area (red rectangle) in the Saint-Lawrence estuary (A; ESRI®). Experimental design (B). UnV: Unvegetated sediment; Veg: vegetated area; N0, N1 and N2: level of nutrient enrichment and targeted value of $NO_x$ concentration.

## 2.2 Sediment collection and maintenance

Experiments were carried out in 2019, during spring in May (immediately after the collapse of fast ice) and summer in August, encompassing, respectively, the beginning of the growing season and the maximum cover of the seagrass meadow. One week before each experiment, 18 sediment cores (10 cm inner diameter, 15 cm long) were collected by hand at low tide using transparent acrylic tubing. Nine sediment cores were collected within three similar (about 2 m of diameter and about 10 cm depth) ice-made tidal pools (3 sediment cores by tidal pool) and the other nine sediment cores were collected within homogeneous vegetated areas 5 m away from the corresponding ice-made tidal pool. Eighteen small sediment cores (2.5 cm inner diameter, 1 cm long) were collected for

sediment grain size and porosity assessment. Each of them was collected next to a large sediment core. The large sediment cores were kept intact and immediately brought back to the laboratory. The sediment cores were left for seven days before starting experiments. During that time and throughout the experiment, sediment cores were supplied with filtered (Ø 50 µm) seawater continuously pumped from the St. Lawrence estuary (6 and 9 °C with a constant salinity of 26 in May and August, respectively, which was like the values measured at the sampling site) to ensure good oxygenation of the overlying water (~1 L per core). A light-dark cycle corresponding to the natural light cycle during the two periods (15 h/ 9 h and 14 h/ 10 h light/dark regime in May and August, respectively) was set with an intensity of about 135 µmol photon $m^{-2}$ $s^{-1}$ which is sufficient to sustain seagrass growth and leaf elongation (Lee et al., 2007).

### 2.3 Experimental design

Large sediment cores were distributed into three treatments, each containing three vegetated sediment cores (hereafter "Veg"), three unvegetated (ice-made tidal pool) sediment cores (hereafter "UnV") and an additional core containing only seawater (Figure 1). Treatments consisted of three fertilisation intensities with one control with no fertilizer addition (hereafter "N0"; 25 µmol $NO_x$ $L^{-1}$) and two fertilizer enriched treatments corresponding to two (hereafter "N1" 50 µmol $NO_x$ $L^{-1}$) and four (hereafter "N2" 100 µmol $NO_x$ $L^{-1}$) times the ambient value of $NO_x$ (see appendix A for realized nutrient enrichment) with N2 corresponding to the average nitrate concentration measured in an coastal agricultural area in the same region (Kamouraska, located 65 km southwest of the study site). Indeed, the average nitrate concentration in the overlying water of tidal marsh of Kamouraska was of 118.8 µmol $NO_x$ $L^{-1}$, on average, with concentrations comprised

The published version can be found at: https://doi.org/10.1016/j.marenvres.2022.105584

between 193.5 and 644.1 µmol $NO_x$ $L^{-1}$ in coastal agricultural drains (Joubert and Bachand, 2012). Fertilizers were applied to each treatment in mesh bags of similar volume placed in the overlying water approximatively five centimeters above the sediment surface so that it allows water circulation and minimizes shadow at the sediment-water interface.

Non-destructive measurements (*i.e.*, length of seagrass leaf, incubations and $O_2$ micro profiles) were performed immediately (hereafter "T0") and 30 days (hereafter "T30") after fertilizer addition. Destructive measurements (*i.e.*, sediment organic matter, pigments content, seagrass biomass, nutrient profiles, macrofauna species composition and bioturbation metrics) were only performed at T30. See Table 1 for a summary of sampling time of each measurement.

The published version can be found at: https://doi.org/10.1016/j.marenvres.2022.105584

Table 1: Summary of measurements and associated sampling time for each seasonal experiment. n = number of sediment core per treatment (combination of *Vegetation* × *Fertilisation intensity*); N = total number of sediment cores

| **Measurement** | **Sampling time** | | | n | **N** |
|---|---|---|---|---|---|
| | *In-situ* | T0 | T30 | | |
| **Sediment characteristics** | | | | | |
| Grain size | X | | | 3 | 18 |
| Porosity | X | | | 3 | 18 |
| SOM | | | X | 3 | 18 |
| Chl *a* | | | X | 3 | 18 |
| Phaeo | | | X | 3 | 18 |
| **Seagrass characteristics** | | | | | |
| Leaf biomass | | | X | 3 | 18 |
| Leaf length | | X | X | 3 | 18 |
| **Macrobenthic community structure** | | | | | |
| Species composition | | | X | 3 | 18 |
| **Bioturbation metrics** | | | | | |
| Porewater exchange rate | | | X | 3 | 18 |
| Sediment reworking | | | X | 3 | 18 |
| **Porewater concentration of solute** | | | | | |
| $O_2$ | | X | X | 1 | 6 |
| Nutrients | | | X | 1 | 6 |
| **Benthic fluxes** | | | | | |
| Fluxes | | X | X | 3 | 18 |

At the beginning and the end of the experiment the length of the five longest seagrass leaves per sediment cores were measured at the nearest mm using a ruler. At the end of the experiment, overlying water just above (~ 1 cm) the sediment surface was sampled. All seagrass leaves were cut for dry biomass assessment in each Veg sediment core. Two grams of surface sediments (*i.e.*, from 0 to 0.5 cm depth) were sampled and stored at – 80 °C for further pigment analysis. Then, all the sediment cores were sliced at

0.5, 1, 1.5, 2, 3, 4, 5, 7 and 10 cm depth below the sediment-water interface. One sediment core per treatment (combination of *Vegetation* × *Fertilisation intensity*) was sliced under $N_2$ atmosphere and each slice was transferred to a 50 mL polyethylene tube. Porewater was then extracted by centrifugation at 5 000 rpm for 15 minutes. After centrifugation, porewater samples were filtered onto 0.2 µm cellulose membrane. Because the porewater volume was too small for nutrient analysis, porewater from the two slices of the first (0-0.5 and 0.5-1 cm slices) and the second (1-1.5 and 1.5-2 cm slices) cm were pooled before being stored at – 20 °C until analysis. After sediment homogenization, about 30 g of sediment from each slice of all sediment cores were individually stored at – 20 °C until sediment organic matter (SOM) and particle mixing analyses. The remaining sediment was sieved onto a 1 mm mesh for benthic macrofauna sampling. Macrofauna samples were preserved in 250 mL of a 4 % buffered formaldehyde solution.

To unravel the mechanisms involved in the response of benthic ecosystems to eutrophication, it is necessary to isolate the effects of nutrient enrichment from inherent covarying environmental factors operating in the field. This ineluctably led to a simplification of natural systems. Therefore, we acknowledge that given the experimental design (*i.e.*, *ex situ* core incubation), there was no potential for macrofauna displacement and thus, the effects of the different fertilisation intensities could only result from differential mortality. We also acknowledge that since incubations were performed in the dark, photosynthetic uptake of nutrient, known to influence sediment biogeochemistry (Marbà et al., 2007), was limited and therefore the measured benthic fluxes may have been overestimated. However, the present results and the literature give clues suggesting that discrepancies between experimental and natural conditions are low. First, previous studies

have shown that seagrasses are able to uptake nutrients in dark conditions (Touchette and Burkholder, 2000). Second, the porewater nutrient concentration profiles in the present study shows differences between vegetated and unvegetated areas, indicating that the influence of seagrass is recorded in the sediment column.

### 2.4 Sediment characteristics

The sediment grain size was assessed by laser diffraction (Malvern Instruments, 2 µm detection limit). The sediment porosity was assessed by measuring the water loss after freeze-drying and corrected for sea salt content. The organic matter content of the sediment was determined as a loss on ignition (% LOI). The freeze-dried samples were combusted at 550 °C for 4 h. Pigments (as proxy of microphytobenthos biomass) were extracted on 2 g of subsamples left in 10 mL of 90 % acetone for 24 h. Subsamples were then centrifuged at 1000 g for 10 min and analyzed fluorometrically (Turner Designs10AU) using an acidification step (5 % HCl) to separate Chl *a* and phaeopigments (Riaux-Gobin and Klein, 1993).

### 2.5 Benthic fluxes

The exchanges of dissolved oxygen and nutrients between the sediment and the water column were used as proxy of benthic-pelagic coupling. Both total and diffusive oxygen fluxes were measured at the sediment-water interface. Diffusive fluxes were considered as a proxy of OM mineralisation and (for $O_2$ and $NO_x$) the reoxidation of reduced chemical species. Total benthic fluxes include, in addition to diffusive fluxes, fauna respiration and sediment irrigation (Glud, 2008). Comparison between total and diffusive fluxes was used to assess the contribution of the macrobenthic community to the ecosystem functioning.

The published version can be found at: https://doi.org/10.1016/j.marenvres.2022.105584

Total benthic fluxes were measured in the dark within each of the sediment cores. When starting measurements, the water flow was turned off and the sediment cores were fitted with PVC lids provided with magnetic stirrers. $O_2$ concentration was measured in real time using an optode (Oxygen sensor Spot SP, PreSens®) connected to an OXY-10 SMA (PreSens®) through optical fibers. Linear calibration was achieved between the oxygen concentration in two solutions of bubbled overlying water (100 %) and sodium ascorbate solution (0 %), respectively. Incubation duration (typically between 2 and 5 h depending on the level of nutrient enrichment) was adjusted so that $O_2$ saturation in the overlying water never fell below 70 %. At the start and the end of incubation, 15 ml of overlying water were sampled and filtered onto 0.2 µm cellulose membrane for further measurement of ammonium ($NH_4^+$) and nitrite + nitrate ($NO_x$). After incubation, sediment cores were opened, and the water flow was turned on until the next measurement. The three additional cores (one for each nutrient enrichment treatment) containing only water were incubated as control. Since no significant temporal changes in $O_2$ and nutrient consumption/production were observed in these controls, the overlying water processes were considered as negligible.

$NH_4^+$ samples were measured by a colorimetric method based on Grasshoff et al. (1999). The precision was ± 5 %. Nitrite + nitrate ($NO_x$ and dissolved inorganic phosphate ($PO_4^{3-}$) were determined by an AutoAnalyzer 3 HR (Seal-analytical®) following Coverly et al. (2009). The errors were < 10 and < 5 % for $NO_x$ and $PO_4^{3-}$, respectively.

During incubation, the $O_2$ depletion in the overlying water was linear. The slope (in mmol $m^{-3}$ $h^{-1}$) from the linear regression of the changes in $O_2$ concentration over incubation duration was used to compute total oxygen uptake (TOU) as follow:

The published version can be found at: https://doi.org/10.1016/j.marenvres.2022.105584

$$TOU = slope \times \frac{V}{A} \quad (1)$$

where $V$ is the volume of overlying water ($m^3$), and $A$ is the surface of the sediment water interface ($m^2$). Assuming linear changes of measured nutrients during incubation as observed for $O_2$, total benthic nutrients fluxes were determined similarly using the slope between the initial and final solute concentration over incubation duration.

Oxygen concentration within the sediment was measured using Clark-type microelectrodes. Five depth profiles of $O_2$ concentration were randomly performed in single cores within each combination of treatments (level of fertilisation intensity × level of vegetation). This sampling design was chosen because of time constraints and because it has been shown that biogeochemical heterogeneity of the sediment is often associated to microenvironment (Stockdale et al., 2009). OX-100 microelectrodes (Unisense®) were piloted using a motor-driven micromanipulator (MU1, Pyroscience®) set up with steps of 200 µm (in May) and 100 µm (in August). Linear calibration was achieved between the oxygen concentration of bubbled overlying water (100 %) and anoxic area of the sediment (0 %). $O_2$ diffusive fluxes (DOU in mmol $m^{-2}$ $h^{-1}$) were assessed with the ProbeFlux program (a modified version of PRO2FLUX software; Deflandre and Duchêne, 2010) using Fick's first law (Eq. (2)).

$$DOU = \phi \times \frac{D_0}{1 - ln(\phi)^2} \times \frac{\delta C}{\delta z} \quad (2)$$

where $\phi$ is the sediment porosity, $D_0$ is the diffusion coefficient ($m^2$ $h^{-1}$) of the element of interest in water (computed from temperature and salinity using *marelac* package on R software; Soetaert and Petzoldt, 2020) and $\frac{\delta C}{\delta z}$ is the concentration gradient (mmol $m^{-3}$ $m^{-1}$). Nutrient diffusive fluxes were predicted from the concentration gradient observed in the

porewater profile using Eq. 2, as previously explained for DOU. They were computed from the concentration in the overlying water just above the sediment-water interface and the concentration in the first cm of the sediment column (porewater extract form the slice 0-0.5 and 0.5-1 cm depth; see section 2.3). Downward $NO_x$ fluxes were computed from NOx concentration in the first cm (porewater extract form the slice 0-0.5 and 0.5-1 cm depth) and in the second cm (porewater extract form the slice 1-1.5 and 1.5-2 cm depth) of the sediment column.

### 2.6 Bioturbation metrics

Bioturbation metrics were used to assess macroinfauna activity. Porewater exchange rates were assessed as a proxy of sediment bioirrigation. They were measured using bromide solute tracer to quantify the volumetric exchange of water and dissolved solutes across the sediment-water interface. Because bromide is a conservative tracer, porewater exchange rates were only assessed at T30. Immediately after benthic flux measurements, 1 mL of the overlying water was sampled and filtered onto 0.2 µm cellulose membrane to assess natural bromide concentration. Then, a known volume of NaBr (1M) was added to each sediment core to reach an initial concentration of about 10 mM in the overlying water. At the start and the end of the incubation. One mL of the overlying water was sampled and filtered onto 0.2 µm cellulose membrane for further bromide analysis. The incubation lasted 24 h, during which constant aeration by air bubbling allowed keeping the overlying water saturated with oxygen and dissolved tracer homogeneously distributed. Samples for bromide ($Br^-$) were analyzed colorimetrically following the method of Lepore and Barak (2009). The concentrations were much higher than the limit of detection and the precision better than 5 %. The porewater exchange rate (Q in L $m^{-2}$ $h^{-1}$) was estimated by

267 computing the bromide flux into the sediment according to Eq. (1) divided by the initial
268 overlying water concentration of excess bromide (mmol $L^{-1}$) (Rao et al., 2014).

269 Sediment reworking was quantified using luminophores as fluorescent sediment
270 particle tracers. One week before the end of the experiment, 5 g of luminophores (125-250
271 µm size range, density = 2.5 g $cm^{-3}$; PARTRAC®) were homogeneously spread at the
272 sediment surface of each sediment core. Luminophores were allowed to settle down for 1h
273 before water flow was turned on. The incubation lasted until the end of the experiment (*i.e.,*
274 7 days). Sediment cores were then sliced (as explained in section 2.3). Sediment slices were
275 freeze-dried and homogenized. For each slice, a subsample of 1 g of dry sediment was
276 photographed under UV light using digital camera ($\alpha$ 9, SONY®). Luminophores were
277 counted on each image after the binarization step (based on RGB threshold) using *Analyze*
278 *particles* function in ImageJ software (ver. 1.53a). The proportions of luminophores in each
279 slice were used to compute depth profiles of luminophores for each sediment cores. The
280 maximum penetration depth of luminophores (MPD as proxy of mixing depth) was
281 assessed from these profiles. Biodiffusion coefficients ($D_b$; as proxy of sediment reworking
282 rate) were estimated by using a simple biodiffusive model (Cochran, 1985) to fit the depth
283 profile of luminophore concentration, following the Eq. (3):

284 $$\frac{\delta^2 C}{\delta t} = D_b \times \frac{\delta^2 C}{\delta z^2} \qquad (3)$$

285 where C is the luminophore concentration (%), t is the time (year), and z is the vertical
286 depth in the sediment column (cm). Modelling was conducted using R software (ver. 4.0.2)
287 (R Core Team, 2020) and relied on *FME* package (Soetaert and Petzoldt, 2010).

The published version can be found at: https://doi.org/10.1016/j.marenvres.2022.105584

### 2.7 Macrofauna identification

Macrofauna were sorted and identified to the lowest possible taxonomic level (typically species) and abundance was determined.

### 2.8 Data analysis

Linear models (LMs; lm function from *stats* package; R Core Team 2020) were fitted to test effects of *Vegetation* (fixed factor, two levels: Veg and UnV), *Fertilisation intensity* (fixed factor, three levels: N0, N1 and N2) and *Month* (fixed factor, two levels: May and August) on sediment characteristics (*i.e.*, sedimentary organic matter, chlorophyll *a* and phaeopigments content) and bioturbation metrics (*i.e.*, porewater exchange rate, maximum penetration depth of luminophore and biodiffusion coefficient) at the end of the experiment. For seagrass leaf' biomass and elongation, LMs were fitted to test the effects of *Fertilisation intensity* and *Month*. Linear Mixed-Effects Models (LMMs; lmer function from *lme4* package; Bates et al., 2015) were fitted by minimizing the Restricted Maximum Likelihood (REML) criterion to assess the effects of *Vegetation*, *Fertilisation intensity*, *Fertilisation duration* (fixed factor, two levels: T0 and T30) and *Month* on diffusive oxygen uptake (DOU) and benthic fluxes. Observations between T0 and T30 were not independent because they were from the same sediment core. To consider natural variability between sediment cores within each treatment and the temporal correlation between observations at T0 and T30, sediment core replicates were considered as a random factor. P-values were obtained by Kenward-Roger F test (with Satterthwaite degrees of freedom) of the full models. Normality and homoscedasticity of the residual were assessed visually. In case normality and/or homoscedasticity of the residual's assumptions were not met (for DOU, OPD and $NH_4^+$ benthic flux), a Box-Cox power transformation of the data

The published version can be found at: https://doi.org/10.1016/j.marenvres.2022.105584

was performed. The effects of *Vegetation*, *Fertilisation intensity* and *Month* on benthic community structure at the end of the experiment were assessed using PERmutational Multivariate ANalyses Of VAriances (PERMANOVAs; adonis2 function from *vegan* package; Oksanen et al., 2019) based on Bray-Curtis dissimilarity coefficient computed from square root transformed macrofauna density data. To visualise the relative differences of significant source of variation, a non-metric multidimensional scaling ordination (nMDS) plot based on Bray-Curtis dissimilarity coefficient was constructed (metaMDS function from *vegan* package; Oksanen et al., 2019). The contribution of individual species to dissimilarity between groups was assess using SIMPER procedure (simper function from *vegan* package; Oksanen et al., 2019). For all analyses, in case of significant effect of factors or interaction between factors ($p < 0.05$), pairwise tests (Tukey contrast for ANOVAs) were performed to characterize their modalities. All figures were built using *ggplot2* package (Wickham, 2016). Table of statistical results are given in appendix B.

# 3 Results

## 3.1 Sediment characteristics

There were significant interactions between *Vegetation, Fertilisation intensity* and *Month* factors in sediment organic matter (SOM) content (Table B. 1). Overall, SOM increased with level of *Fertilisation intensity* and this increase was greater in UnV than in Veg and in August than in May (Table 2). There were significant interactions between *Vegetation, Fertilisation intensity* and *Month* factors in sediment chlorophyll *a* (Chl *a*) content. In UnV, Chl *a* content increased with level of *Fertilisation intensity* during both May and August experiments. In Veg, Chl *a* content increased with level of *Fertilisation intensity* during May experiment but to a lower extend than in UnV. Chl *a* content remains

The published version can be found at: https://doi.org/10.1016/j.marenvres.2022.105584

334 relatively stable over level of *Fertilisation intensity* in August experiment. There were
335 significant interactions between *Vegetation, Fertilisation intensity* and *Month* factors in
336 sediment phaeopigment content. Overall, phaeopigment increased with level of
337 *Fertilisation intensity* and this increase was greater in Veg than in UnV and in August than
338 in May. The Chl *a* / (Phaeo + Chl *a*) ratio (as proxy of SOM degradation) was relatively
339 high and relatively stable over the *Fertilisation intensity* levels in both UnV and Veg during
340 May experiment. During the August experiment, the Chl *a* / (Phaeo + Chl *a*) ratio was
341 relatively stable over level of *Fertilisation intensity* in UnV but decreased in Veg.
342

The published version can be found at: https://doi.org/10.1016/j.marenvres.2022.105584

Table 2: *Sediment characteristics.* Mean (± SE) sedimentary organic matter (SOM in % LOI), chlorophyl *a* (Chl *a* in µg $g^{-1}$), phaeopigment (Phaeo in µg $g^{-1}$), Chl *a* / Phaeopigment ratio (Chl *a* / (Phaeo + Chl *a*)), seagrass leaf biomass (g) and seagrass leaf elongation (cm $day^{-1}$) for each combination of *Month*, *Fertilisation intensity* and *Vegetation*.

| | | | **SOM** | **Chl *a*** | **Phaeo** | **Chl *a* / (Phaeo + Chl *a*)** | **Seagrass leaf biomass** | **Seagrass leaf elongation** |
|---|---|---|---|---|---|---|---|---|
| May | N0 | UnV | 2.83 ± 0.25 | 13.36 ± 0.14 | 1.85 ± 0.01 | 0.88 ± 0.00 | -- | -- |
| | | Veg | 1.61 ± 0.04 | 11.79 ± 0.12 | 1.68 ± 0.05 | 0.88 ± 0.00 | 0.32 ± 0.02 | 0.30 ± 0.00 |
| | N1 | UnV | 2.89 ± 0.33 | 27.82 ± 2.08 | 3.23 ± 0.58 | 0.90 ± 0.01 | -- | -- |
| | | Veg | 2.02 ± 0.15 | 22.70 ± 1.37 | 3.05 ± 0.50 | 0.88 ± 0.02 | 0.37 ± 0.02 | 0.44 ± 0.01 |
| | N2 | UnV | 5.19 ± 0.09 | 55.01 ± 0.48 | 3.96 ± 0.85 | 0.93 ± 0.01 | -- | -- |
| | | Veg | 2.96 ± 0.17 | 31.11 ± 1.53 | 3.26 ± 0.15 | 0.90 ± 0.00 | 0.06 ± 0.03 | 0.00 ± 0.08 |
| August | N0 | UnV | 2.61 ± 0.18 | 16.96 ± 1.53 | 6.91 ± 0.77 | 0.71 ± 0.04 | -- | -- |
| | | Veg | 3.80 ± 0.12 | 10.14 ± 1.59 | 9.63 ± 0.22 | 0.51 ± 0.04 | 1.97 ± 0.05 | -0.01 ± 0.01 |
| | N1 | UnV | 3.91 ± 0.06 | 26.89 ± 2.70 | 9.80 ± 0.86 | 0.73 ± 0.02 | -- | -- |
| | | Veg | 4.01 ± 0.09 | 11.66 ± 0.69 | 17.60 ± 0.01 | 0.40 ± 0.01 | 1.96 ± 0.03 | -0.02 ± 0.01 |
| | N2 | UnV | 6.41 ± 0.02 | 53.62 ± 3.49 | 12.82 ± 0.67 | 0.81 ± 0.01 | -- | -- |
| | | Veg | 5.63 ± 0.25 | 11.73 ± 1.46 | 30.22 ± 1.78 | 0.28 ± 0.03 | 1.83 ± 0.08 | 0.00 ± 0.05 |

The published version can be found at: https://doi.org/10.1016/j.marenvres.2022.105584

Seagrass leaf biomass significantly differed between *Fertilisation intensity* and *Month* factors (Table B. 2). Overall, leaves biomass was lower in May than in August and higher in N0 and N1 than in N2 (Table 2). Seagrass leaf elongation significantly differed between *Fertilisation intensity* and *Month* with a significant interaction between these two factors. Leaf's elongation occurred only in May and was higher in N1 intermediate in N0 and barely detectable in N2.

### 3.2 Macrobenthic community structure

The non-metric multidimensional scaling (nMDS) suggested that species assemblages differed between months and levels of vegetation but were not influenced by the fertilisation (Figure 2). This was confirmed by PERMANOVA results with a significant interaction between Vegetation and Month factors in macrobenthic community structure (Table B. 3). The difference in community structure between May and August experiments was mainly due to the substantial increase in the densities of Tellinid Bivalve *L. balthica* in UnV and Veg and of Gastropoda (*i.e.*, *E. truncata* and *Littorina saxatilis*) in Veg (Table 3). The significant difference between UnV and Veg in August was mainly due to larger densities of Gastropoda in Veg (Table 3).

The published version can be found at: https://doi.org/10.1016/j.marenvres.2022.105584

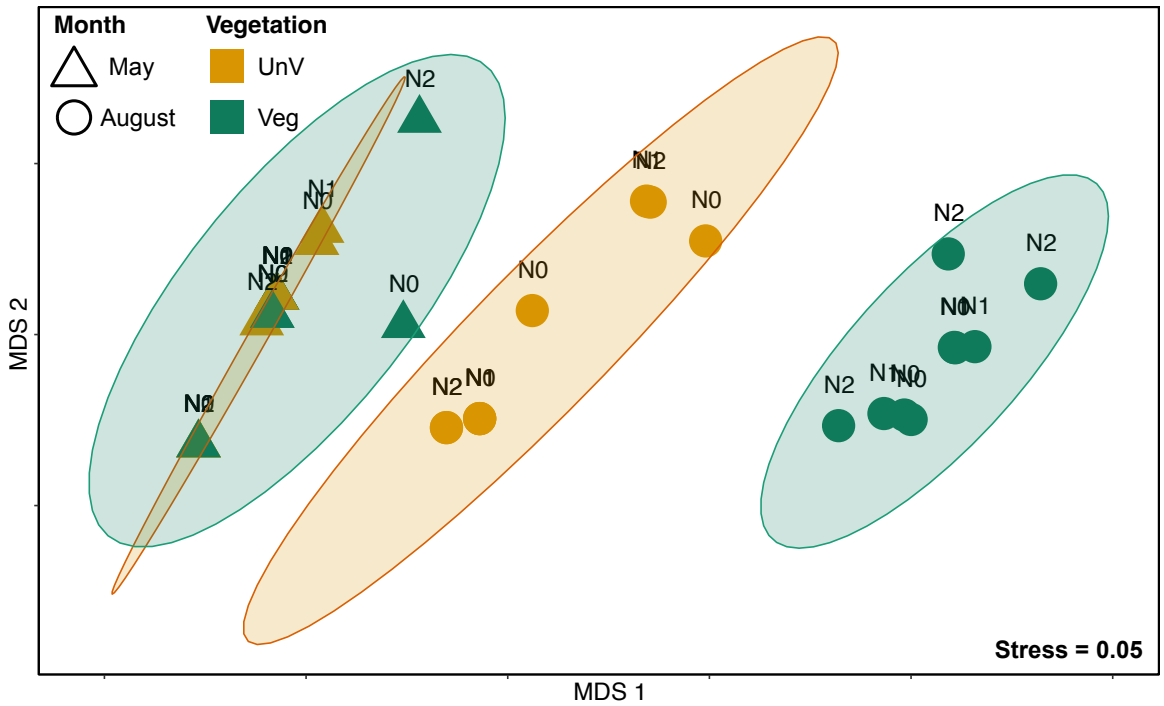


Figure 2: *Community structure*. Non-metric multidimensional scaling ordination of macrofauna composition based on density data. UnV: Unvegetated area, Veg: Vegetated area. N0, N1 and N2 represent the level of fertilisation intensity. Ellipses represent the standard deviation of points in each combination of Month × Vegetation factors. PERMANOVA analysis indicates significant interaction between Month and Vegetation factors (see table B.3)

The published version can be found at: https://doi.org/10.1016/j.marenvres.2022.105584

Table 3: *SIMPER analyses*. List of species with their mean densities (ind. $m^{-2}$) and cumulative contribution to dissimilarity between groups. UnV: unvegetated areas, Veg: vegetated areas.

| | | Species | Density | | Cumulative contribution to dissimilarity |
|---|---|---|---|---|---|
| **Between levels of Vegetation** | | | **UnV** | **Veg** | |
| | Within May | *Mya arenaria* | 183.9 | 141.47 | 60.85 |
| | | *Hediste diversicolor* | 169.8 | 183.91 | 92.89 |
| | | *Limecola balthica* | 0 | 14.15 | 100 |
| | | *Littorina saxatilis* | 0 | 0 | 100 |
| | | *Ecrobia truncata* | 0 | 0 | 100 |
| | Within August | *Ecrobia truncata* | 14.15 | 3098.22 | 37.1 |
| | | *Littorina saxatilis* | 0 | 2235.24 | 72.41 |
| | | *Limecola balthica* | 396.12 | 1881.57 | 90.72 |
| | | *Hediste diversicolor* | 84.88 | 56.59 | 95.57 |
| | | *Mya arenaria* | 56.59 | 56.59 | 100 |
| **Between levels of Month** | | | **May** | **August** | |
| | Within UnV | *Limecola balthica* | 0 | 396.12 | 56.77 |
| | | *Mya arenaria* | 183.9 | 56.59 | 82.36 |
| | | *Hediste diversicolor* | 169.8 | 84.88 | 96.81 |
| | | *Ecrobia truncata* | 0 | 14.15 | 100 |
| | | *Littorina saxatilis* | 0 | 0 | 100 |
| | Within Veg | *Ecrobia truncata* | 0 | 3098.22 | 31.5 |
| | | *Littorina saxatilis* | 0 | 2235.24 | 61.8 |
| | | *Limecola balthica* | 14.15 | 1881.57 | 89.22 |
| | | *Hediste diversicolor* | 183.91 | 56.59 | 95.14 |
| | | *Mya arenaria* | 141.47 | 56.59 | 100 |

### 3.3 Bioturbation metrics

Porewater exchange rate (Q) ranged from 0.03 (in Veg, N0 in May) to 6.0 L $m^{-2}$ $h^{-1}$ (in Veg, N2 in August). There was a significant interaction between *Vegetation* and *Fertilisation intensity* factors (Table B. 4). Q increased by a factor 5.1 between N0 and N2 in Veg and by a factor 2.2 in UnV (Figure 3A). There was also a significant interaction between *Fertilisation intensity* and *Month* factors. Although it tended to increase with nutrient enrichment, Q did not significantly differ between levels of *Fertilisation intensity*

in May (0.8 ± 0.3, 1.5 ± 0.2 and 1.7 ± 0.2 L $m^{-2}$ $h^{-1}$ in N0, N1 and N2, respectively) (Data not depicted in figure). On the contrary, Q was minimum in N0 (1.3 ± 0.2 L $m^{-2}$ $h^{-1}$), intermediate in N1 (3.3 ± 0.4 L $m^{-2}$ $h^{-1}$) and maximum in N2 (4.7 ± 0.4 L $m^{-2}$ $h^{-1}$) in August (Data not depicted in figure). Q was similar between May and August in N0 and lower in May than in August in N1 and N2.

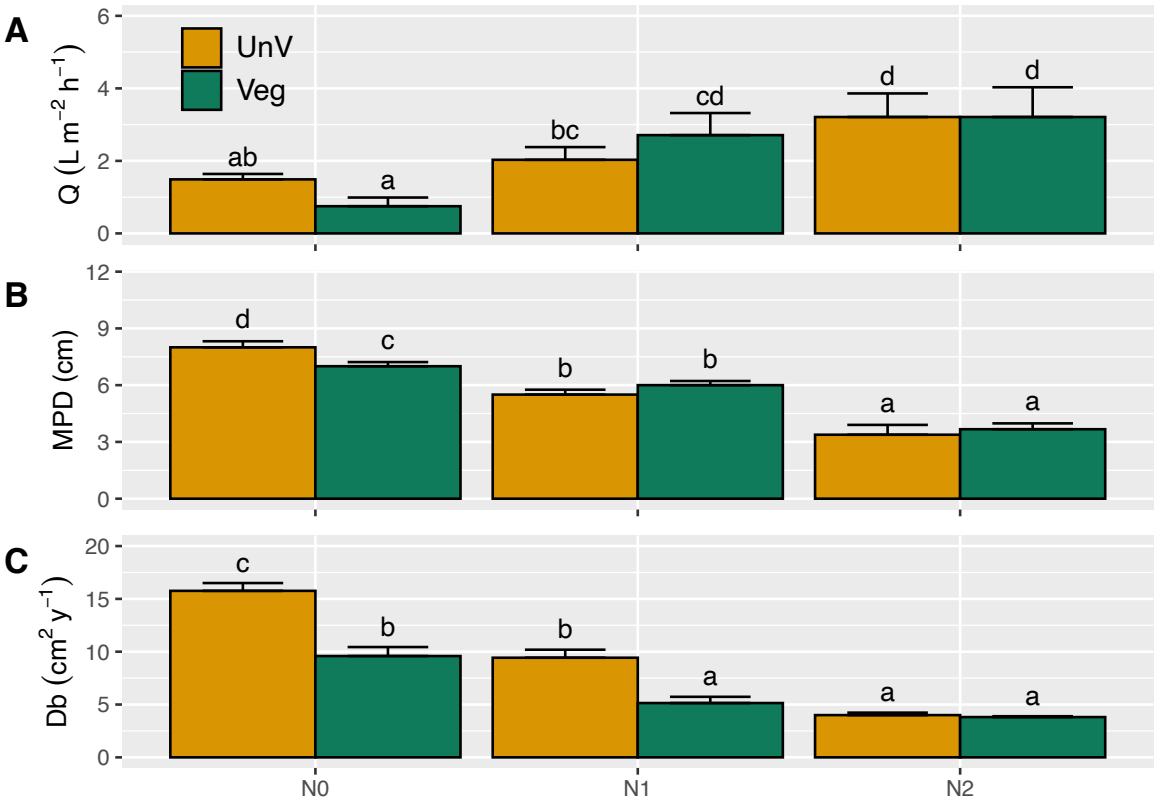


Figure 3: *Bioturbation metrics*. Mean (± SE) (A) porewater exchange rate (Q in mL $m^{-2}$ $h^{-1}$), (B) maximum penetration depth of luminophores (MPD in cm) and (C) biodiffusion coefficient ($D_b$ in $cm^2$ $year^{-1}$) for N0, N1 and N2 within level of *Vegetation* (averaged over the levels of *Month* factors) Different letters indicate significant ($p < 0.05$) differences.

The maximum penetration depth of luminophores (MPD) ranged from 1.75 (in UnV, N2 in August) to 9 cm (in UnV, N0 in August). There was a significant interaction between *Vegetation* and *Fertilisation intensity* factors (Table B. 4). MPD decreased by a factor 2.4 between N0 and N2 in UnV and by a factor 1.9 in Veg (Figure 3B). In the absence of fertilisation (N0), MPD was 1.1 time deeper in UnV than in Veg. MPD did not significantly differ between these two treatments in N1 nor N2. There was also a significant

interaction between *Month* and *Fertilisation intensity* factors. During both May and August experiments, there was a decrease of MPD with increasing fertilisation intensity (Data not depicted in figure). MPD was significantly deeper in August than in May in the absence of nutrient enrichment (8 ± 0.3 *vs* 7 ± 0.2 cm, respectively), similar between these two months in N1 (5.8 ± 0.2 *vs* 5.7 ± 0.3 cm, respectively) and significantly shallower in August than in May in N2 (2.9 ± 0.4 *vs* 4.2 ± 0.2 cm, respectively).

The biodiffusion coefficient ($D_b$) ranged from 3.61 (in UnV, N2 in August) to 17.43 $cm^2\ y^{-1}$ (in UnV, N0 in August). $D_b$ significantly differed between *Vegetation* and *Fertilisation intensity* with a significant interaction between these two factors (Table B. 4). Overall, there was a decrease of $D_b$ with increasing fertilisation intensity (Figure 3C). In UnV, $D_b$ were 1.7 time higher in N0 than in N1 and 2.4 times higher in N1 than in N2. In Veg, $D_b$ were 1.9 time higher in N0 than in N1 and did not significantly differ between N1 and N2. $D_b$ were 1.6 and 1.8 time higher in UnV than in Veg in N0 and N1, respectively, and similar in N2.

### 3.4 Oxygen and nutrients pore water concentration

The oxygen penetration depth (OPD) ranged from 1.4 (at T30 in UnV, N2 in August) to 8.4 mm (at T0 in Veg, N0 in May). There was a significant interaction between *Vegetation*, *Fertilisation intensity* and *Fertilisation duration* factors in OPD (Table B. 5). At T0, OPD were similar between levels of *Vegetation* and *Fertilisation intensity* factors (Figure 4A). At T30, OPD tended to decrease with levels of *Fertilisation intensity* in UnV and was reduced by a factor 1.6 in N2 as compared to N0. In Veg, OPD were similar between N0 and N1 and was reduced by a factor 1.5 in N2 as compared to N0.

The published version can be found at: https://doi.org/10.1016/j.marenvres.2022.105584

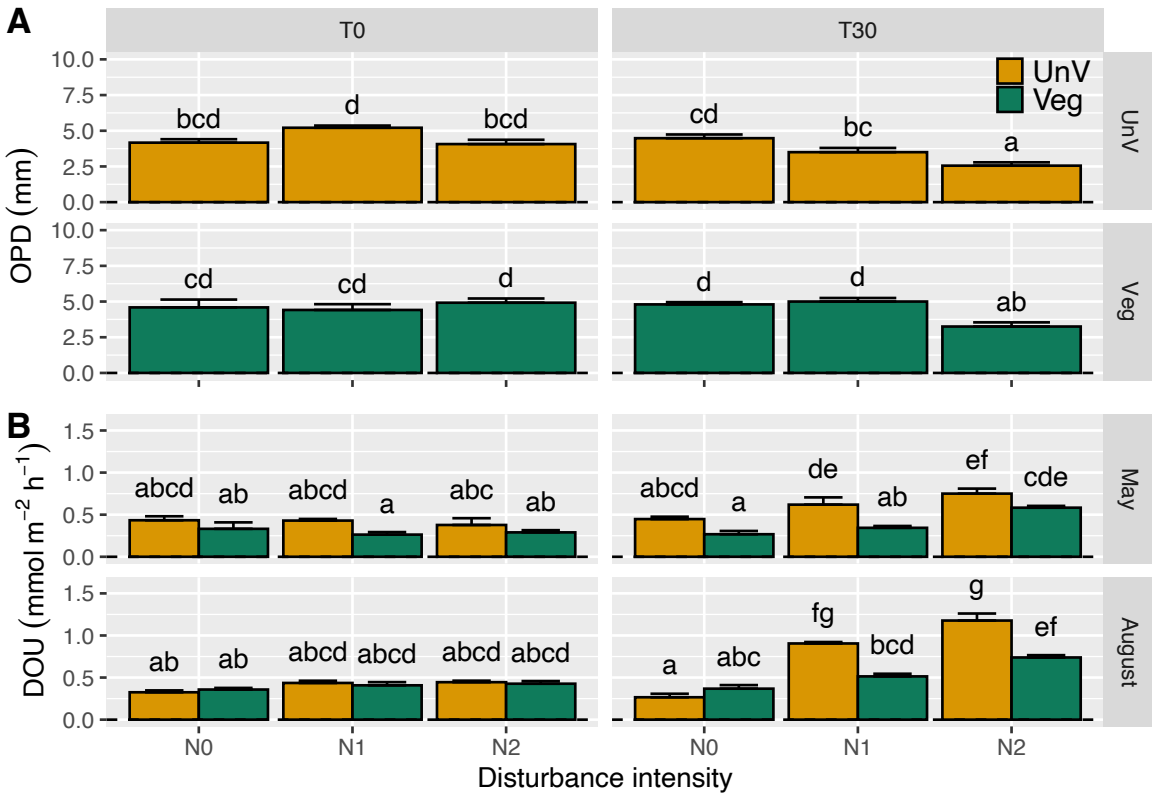


Figure 4: *Oxygen dynamics*. Mean (± SE) (A) oxygen penetration depth (OPD) for unvegetated (UnV) and vegetated (Veg) areas averaged over level of *Month* and (B) diffusive oxygen uptake (DOU) at the sediment-water interface for UnV and Veg at different level of *Fertilisation intensity* (N0, N1 and N2) and *Fertilisation duration* (T0 and T30) in May and in August. Different letters indicate significant differences ($p < 0.05$) between levels of factors.

The diffusive oxygen uptake (DOU) ranged from 0.1 (at T30, in UnV, N0 in August) to 1.4 mmol $m^{-2}$ $h^{-1}$ (at T30, in UnV, N2 in August). The DOU significantly differed between *Vegetation*, *Fertilisation intensity*, *Fertilisation duration* and *Months* with significant interaction between these four factors (Table B. 5). At T0, DOU were similar between levels of *Vegetation* and *Month* factors (Figure 4B) and DOU in N0 were similar between T0 and T30 in both May and August experiments. At T30, DOU tended to increase with levels of *Fertilisation intensity*. This increase was greater in UnV than in Veg and in August than in May.

Porewater profiles of measured $NH_4^+$, $NO_x$ and $PO_4^{3-}$ at the end of the experiment are shown in Figure 5. Overall, there was an increase in $NH_4^+$ concentrations with depth

435 which were greater in N2 than in N1 and in N1 compared to N0. In May, $NH_4^+$
436 concentration increase was almost linear in N0 with a greater increase in Veg than in UnV.
437 $NH_4^+$ concentration increase in N1 was greater in UnV than in Veg. In N2, $NH_4^+$
438 concentration increase was similar between Veg and UnV. In August, $NH_4^+$ concentration
439 increase was also almost linear in N0 with a greater increase in UnV than in Veg. In N1
440 and N2, $NH_4^+$ concentration increased rapidly between the sediment surface and 2.5 to 3.5
441 cm depth and then steadily increase with depth.

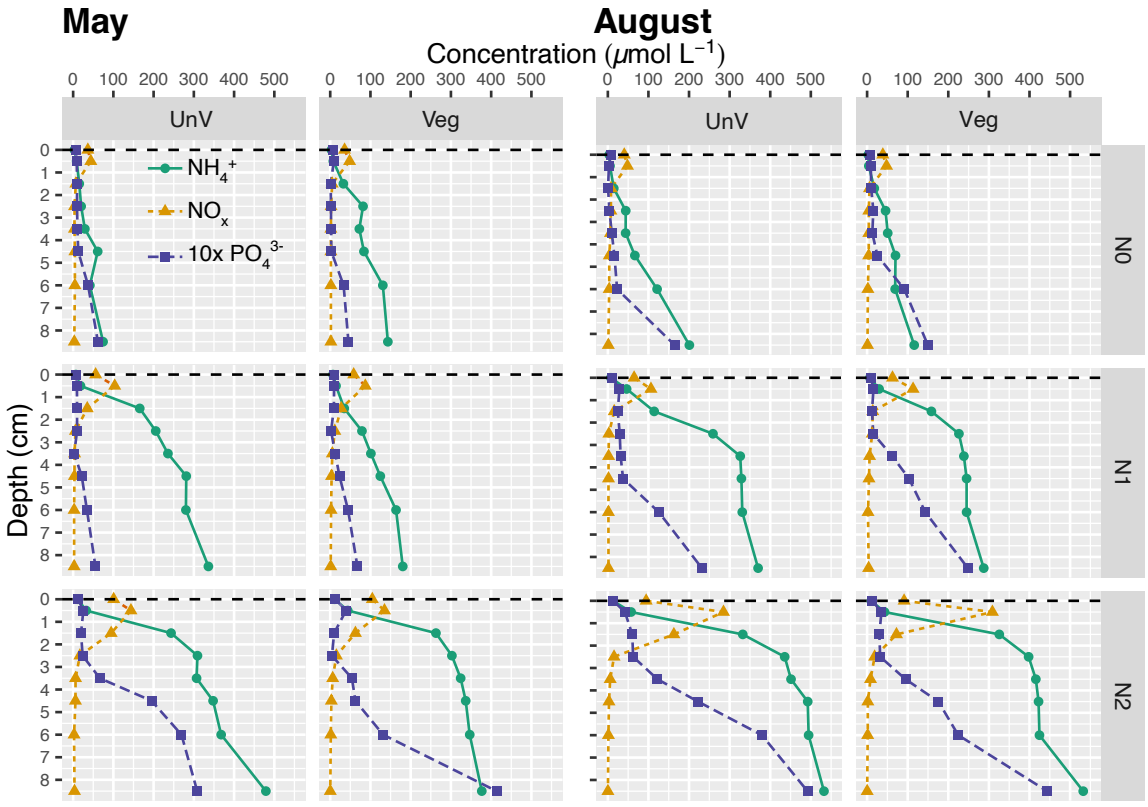


442
443 Figure 5: *Nutrient profiles*. Porewater profiles of $NH_4^+$ (green circles and line), $NO_2 + NO_3^-$ ($NO_x$; orange
444 triangles and dotted line) and 10 × $PO_4^{3-}$ (purple squares and dashed line) for each level of nutrient
445 enrichment (N0, N1 and N2) at the end of the experiment in unvegetated (UnV) and vegetated (Veg) sediment
446 cores during May and August experiments.

447 In every treatment, a peak of $NO_x$ occurred at 0.5 cm depth. $NO_x$ concentration at
448 0.5 cm was similar between UnV and Veg for each level of *Fertilisation intensity* and
449 increased with level of *Fertilisation intensity* with a maximum in N2 in August. Below

0.5 cm, $NO_x$ was then rapidly consumed as indicated by the steep decrease in $NO_x$ concentrations that drop to near 0 µmol $L^{-1}$ (< detection limit).

$PO_4^{3-}$ porewater concentration profiles were similar between UnV and Veg treatments with porewater concentrations barely detectable close to the sediment surface and then an increase with depth. The depth at which $PO_4^{3-}$ porewater concentration start to increase decreased with level of *Fertilisation intensity* and was of 4.5, 3.5 and 2.5 cm in N0, N1 and N2, respectively. Overall, $PO_4^{3-}$ porewater concentration tended to be higher in August than in May.

To visually assess the proportion of total flux corresponding to diffusive flux, nutrient diffusive fluxes computed from nutrient profiles are shown as black points in Figure 6 (except $PO_4^{3-}$ fluxes which were barely detectable). Upward $NH_4^+$ diffusive fluxes through the sediment-water interface were relatively low (< 1 mmol $m^{-2}$ $h^{-1}$) in N0 at both May and August experiments. $NH_4^+$ diffusive fluxes increased with nutrient enrichment and this increase was higher in August (33.3 and 28.0 times higher in N2 than in N0 for UnV and Veg, respectively) than in May (5.3 and 8.0 times higher in N2 than in N0 for UnV and Veg, respectively). In May, the upward diffusive fluxes of $NH_4^+$ accounted for the totality of total fluxes measured in core incubations. In August, it also accounted for the totality of total fluxes in N0, but only to 88 and 33 % of total fluxes in N1 in UnV and Veg, respectively and 81 and 20 % of total fluxes in N2 in UnV and Veg, respectively. The upward $NO_x$ diffusive fluxes at the sediment-water interface were low in N0 at both May and August experiments. As for NH4+, $NO_x$ diffusive fluxes increased with nutrient enrichment and this increase was higher in August (33.7 and 27.3 times higher in N2 than in N0 for UnV and Veg, respectively) than in May (8.1 and 2.8 times higher in N2 than in

N0 for UnV and Veg, respectively). In May, $NO_x$ diffusive fluxes accounted for the totality of total fluxes. In August, however, it accounted for 100% of total fluxes in N0, the totality and 32 % of total fluxes in N1 in UnV and Veg, respectively and finally, it represented only 77 % of total fluxes in N2 in both UnV and Veg. $NO_x$ consumption was also computed from 0.5 to 1.5 cm depth with sharp downward fluxes just below the maxima. These downward NOx diffusive fluxes tended to be lower in UnV than in Veg in N0 in both May and August experiments (0.8 and 1.1 in May and 1.0 and 1.2 mmol $m^{-2}$ $h^{-1}$ in August, respectively). $NO_x$ consumption increased with nutrient enrichment and this increase was higher in August than in May (1.5 and 2.1 in May and 4.2 and 7.4 mmol $m^{-2}$ $h^{-1}$ in August for N2 in UnV and Veg, respectively). The upward diffusive fluxes of $PO_4^{3-}$ were barely detectable (< 0.1 mmol $m^{-2-}$ $h^{-1}$) in all treatment and in May and August (data not shown).

### 3.5 Total benthic fluxes

Total benthic fluxes of $O_2$, $NH_4^+$ and $NO^x$ fluxes are shown in Figure 6. $PO_4^{3-}$ fluxes were barely detectable and are not shown. All total fluxes were similar between levels of *Fertilisation intensity* at T0 during both May and August experiments. Total fluxes in N0 were also similar between T0 and T30 during both May and August experiments.

The published version can be found at: https://doi.org/10.1016/j.marenvres.2022.105584

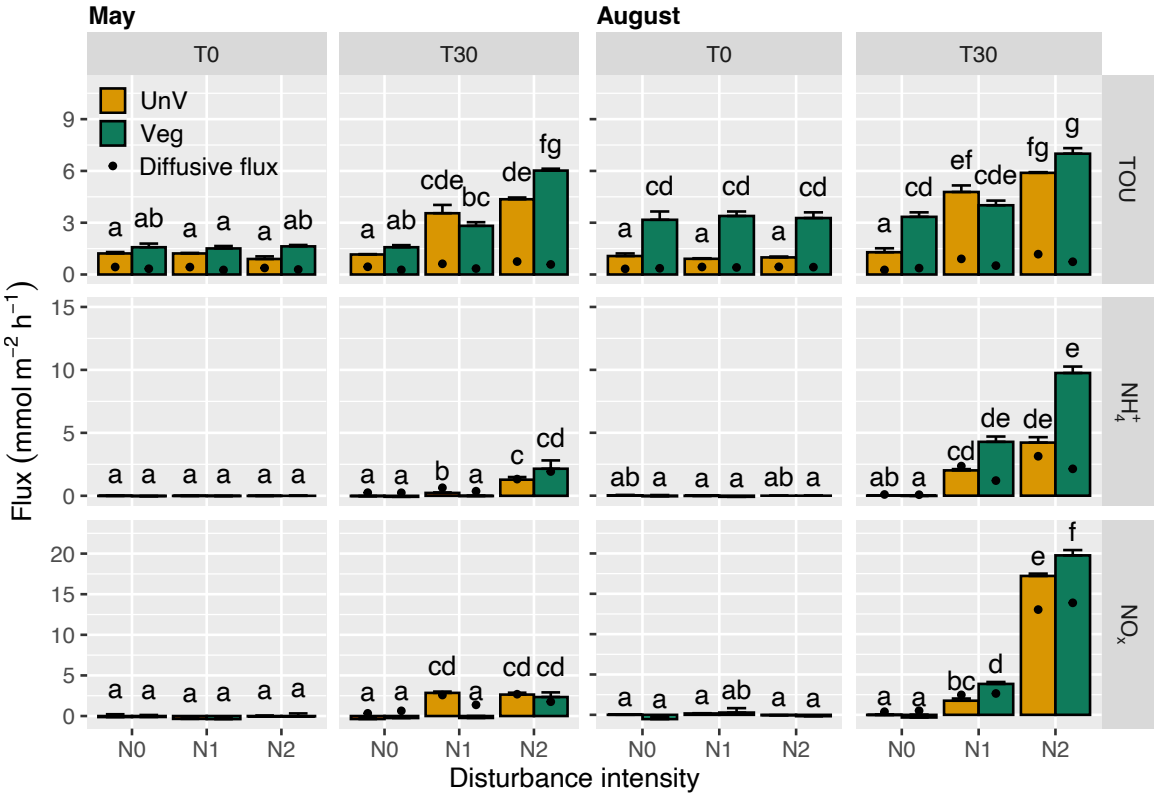


Figure 6: *Benthic fluxes*. Mean (± SE) total oxygen uptake (TOU) and total nutrients ($NH_4^+$ and $NO_x$) fluxes at the sediment-water interface for unvegetated (UnV in orange) and vegetated (Veg in green) areas at distinct levels of Fertilisation intensity (N0, N1 and N2) and Fertilisation duration (T0 and T30) in May and August. Black points depict the mean diffusive fluxes of the corresponding element. Different letters indicate significant differences ($p < 0.05$) assessed by pairwise comparisons for the interaction factor *Vegetation* × *Fertilisation intensity* × *Fertilisation duration* × *Month.*

There was a significant interaction between *Vegetation*, *Fertilisation intensity*, *Fertilisation duration* and *Month* in TOUs (Table B. 6). During May experiment at T30, TOUs were higher in N1 and N2 than in N0 for UnV. For Veg, TOUs were significantly in N2 higher than in N0 and N1. During August experiment, TOUs were significantly higher in N2 and N1 than in N0 for UnV. For Veg, TOUs were significantly in N2 higher than in N0 and N1.

There was significant interaction between *Vegetation*, *Fertilisation intensity*, *Fertilisation duration* and *Month* in $NH_4^+$ fluxes (Table B. 6). During May experiment at T30, $NH_4^+$ fluxes were barely detectable in N0, intermediate in N1 and higher in N2 for UnV. For Veg, $NH_4^+$ fluxes were significantly in N2 higher than in N0 and N1. During

The published version can be found at: https://doi.org/10.1016/j.marenvres.2022.105584

August experiment, $NH_4^+$ fluxes were significantly higher in N2 and N1 than in N0 for both UnV and Veg. Although not significant, $NH_4^+$ fluxes tended to be higher in N2 than in N1 for both UnV and Veg. Overall, the effect of *Fertilisation intensity* on $NH_4^+$ fluxes was greater in August than in May.

There was significant interaction between *Vegetation*, *Fertilisation intensity*, *Fertilisation duration* and *Month* in $NO_x$ fluxes (Table B. 6). During the May experiment at T30, $NO_x$ fluxes were barely detectable in N0 than in N1 and N2 for UnV. For Veg, $NO_x$ fluxes were significantly in N2 higher than in N0 and N1. During the August experiment, $NO_x$ fluxes were barely detectable in N0, intermediate in N1 and higher in N2 for both UnV and Veg. The effect of *Fertilisation intensity* on $NO_x$ fluxes was greater in Veg than in UnV. Overall, the effect of *Fertilisation intensity* on $NO_x$ fluxes was greater in August than in May.

## 4 Discussion

Over the last decades, the oversupply of N-nutrients in commonly N-limited ecosystems has led to eutrophication in many coastal ecosystems (Rabalais et al., 2009). Using *ex-situ* experiments, a powerful tool for the detailed study of the response of the benthic ecosystem to a specific disturbance in a controlled system, this study aimed at unravelling benthic ecosystem processes that may mitigate or favour eutrophication. We showed that nutrient enrichment of the overlying water triggered changes in the quantity and quality of SOM with cascading effects on early diagenetic processes deeper in sediment column, on macrobenthic community structure and activity and finally, on the benthic fluxes.

The published version can be found at: https://doi.org/10.1016/j.marenvres.2022.105584

### 4.1 Changes in the quantity and quality of organic matter

The similar increase in the quantity of sediment pigments (as a proxy of microphytobenthos) and organic matter (SOM) content in enriched treatments suggested that (i) nutrient limitation occurred at the study site and (ii) SOM content depended to a significant extent on microphytobenthos. Microphytobenthos play a key role in shallow ecosystem functioning, contributing to primary production, being a preferred food source for deposit-feeding macrofauna (Miller et al., 1996) and influencing solute fluxes at the sediment-water interface (Hope et al., 2020). Therefore, the increase of microphytobenthos biomass associated with nutrient enrichment can profoundly alter ecosystem functioning (Hope et al., 2020). The larger increase of sediment pigments and organic matter content in in unvegetated than in vegetated areas is consistent with the results of previous studies showing that seagrass can filter nutrients from the water column (*e.g.*, Asmala et al., 2019), especially during the growing season, thus reducing the pool of available nutrients for microphytobenthos and other primary producers. The presence of seagrass leaves, particularly in August when the leaf biomass was maximum, may also have shaded the sediment surface, thus limiting light availability to microphytobenthos.

The degradation of organic matter (depicted by the Chl *a* / (Phaeo + Chl *a*) ratio) was larger in August than in May and was larger in vegetated than in unvegetated areas in August. This is consistent with the higher density of macrofauna, particularly the occurrence of grazers (*e.g.*, *L. saxatilis*, *E. truncata*) in August, especially in vegetated area, which fed on microphytobenthos. In addition, the shading of sediment surface by seagrass leaves could explain a higher pigment degradation in vegetated areas (Veuger and van Oevelen, 2011). In August, the relatively stable Chl *a* / (Phaeo + Chl *a*) ratio in

551 unvegetated area, suggested that the increase of Chl *a* content was offset by grazing
552 pressure. On the contrary, pigment degradation increased over levels of nutrient enrichment
553 in vegetated areas. Given that seagrass leaves biomass decreased with nutrient enrichment
554 (Table 2), the pigment degradation was most likely due to a substantial increase of
555 macrofauna grazing pressure on microphytobenthos rather than an increase of shading
556 effect by seagrass leaves. It is also possible that senescent epiphytes contributed to the
557 increase of phaeopigment content in the sediment of vegetated areas.

558 **4.2 Changes in early diagenetic processes**

559 Overall, the oxygen penetration depth (OPD) tended to decrease while diffusive
560 oxygen uptake (DOU) tended to increase in enriched treatments. Oxygen is the most
561 favorable electron acceptor available for organic matter mineralisation and oxidation of
562 reduced chemical species (Glud, 2008). Therefore, our results of OPD and DOU are
563 consistent with the increase of SOM and the higher concentration of reduced chemical
564 species in porewater in enriched treatments. It is worth noting that DOU tended to be larger
565 and triggered by a lower level of fertilisation in unvegetated than in vegetated areas,
566 suggesting that, regarding DOU, unvegetated areas were more sensitive to nutrient
567 enrichment than vegetated areas.

568 At the end of May and August experiments, the nutrient profiles in enriched
569 treatments differed from the control over the whole sampled sediment column (*i.e.*, from 0
570 to 10 cm depth) in both unvegetated and vegetated areas. This result showed that the effects
571 of nutrient enrichment of the overlying water cascade deeper into the sediment column.
572 The substantial increases in $NH_4^+$ porewater concentration in enriched treatments were
573 most likely due to the mineralization of the oversupply of SOM at the sediment-water

574 interface (see Table 2) and bioturbation processes which allow the transport of OM deep
575 within the sediment column (Kristensen et al., 2012). In the intermediate level of
576 fertilisation porewater $NH_4^+$ concentration was lower in vegetated than in unvegetated
577 areas during both May and August experiments. These discrepancies can be linked with
578 the growth of seagrass since $NH_4^+$ is their main source of inorganic nitrogen (Lee et al.,
579 2007). Interestingly, the difference in porewater $NH_4^+$ concentrations between the control
580 and the intermediate level of fertilisation in vegetated areas was lower in May than in
581 August. This is in good agreement with the growth period (typically beginning in May to
582 reach a maximum of leaves biomass in August) of seagrass in the study area (Pascal et al.,
583 2020). This result suggested that, within tolerance level, seagrass buffered the effect of
584 nutrient enrichment by reducing the pool of available $NH_4^+$.

585 The peak of $NO_x$ (0-1 cm depth) largely increased in concentration in enriched
586 treatments, indicating an enhancement of nitrification process which was not balanced by
587 an enhancement of $NO_x$ assimilation or reduction processes. Below 0.5 cm $NO_x$ porewater
588 concentration decreased sharply. This was probably due to the occurrence nitrate reduction
589 processes (*e.g.*, denitrification, ANAMMOX, DNRA). The occurrence of these processes
590 was consistent with the OPD of about 0.5 cm depth measured during this study (Figure 4).
591 Overall, nitrate reduction processes were more efficient in enriched treatments, as
592 suggested by the computation of $NO_x$ consumption between 0.5 and 1.5 cm. However, our
593 study did not allow to discriminate the different nitrate reduction processes occurring here
594 and it should prove interesting to further undertake studies using isotope pairing techniques
595 (Nielsen, 1992; Song et al., 2013) in addition to the measurement of dissolved manganese
596 and iron to unravel nitrogen cycling in nutrient enriched sediment.

$PO_4^{3-}$ porewater concentration in the first cm of the water column was barely detectable in all treatments. In the top layers of the sediment, the presence of iron-oxides usually trapped phosphate in the particulate phase (Slomp, 2012). At depth, the reductive dissolution of iron-oxides release dissolved $PO_4^{3-}$ in porewater which can thus diffuse toward the overlying water (Anschutz et al., 2007; Slomp, 2012). The depth at which $PO_4^{3-}$ was released in porewater was shallower in enriched treatment. Interestingly, the depths at which $PO_4^{3-}$ was released are consistent with the thickness of the mixing layer (Figure 3B), suggesting that adsorption capacity of $PO_4^{3-}$ by the sediment was controlled by the transport of iron-oxide at depth through bioturbation. Overall, our results suggested an accumulation of reduced chemical species in the porewater, building up the "oxygen debt" of the sediment

### 4.3 Changes in seagrass health

In May, seagrass leaf elongation was the highest in the intermediate level of fertilisation, suggesting that the growth of seagrass was nutrient limited. The biomass and elongation of seagrass leaf were altered in the highest level of fertilisation. This can be explained by three mechanisms. First, the increase of reduced chemical species (as suggested by the increase of $NH_4^+$ and $PO_4^{3-}$ porewater concentration; Figure 5) can be toxic for seagrass in high concentrations (Touchette and Burkholder, 2000; Van Der Heide et al., 2008). Second, the increase of epiphytes loads in nutrient enriched treatment during both May and August experiment (personal observations) compete with seagrass for light and carbon (Noisette et al., 2020). Third, water column $NO_3^-$ enrichment may directly cause imbalance of carbohydrate (Burkholder et al., 1992). Overall, the decrease of seagrass health can have far reaching effect by decreasing the radial $O_2$ loss from roots (Brodersen

et al., 2015) and thus eases the accumulation of toxic reduced chemical species within the sediment column.

### 4.4 Changes in community structure and activity

Nutrient enrichment typically triggered changes in benthic community structure due to an increase of OM which may cause hypoxia (Diaz and Rosenberg, 2008). During this study, nutrient enrichment did not significantly alter the macrobenthic community structure. This was probably due to the presence of sea ice during wintertime. Indeed, the presence of sea ice causes the mortality or displacement of benthic organisms (typically the organisms living at the sediment surface or in the first cm of the sediment column) which are not able to cope with such harsh environmental conditions (Pascal et al., 2020). Thus, sea ice disturbance may already have removed sensitive species. Sea ice disturbance also explain the low diversity observed during this study or in natural environment in a similar high latitude seagrass meadow (Pascal et al., 2020). Relatively low diversity and abundance has already been reported in the Baltic Sea (Bonsdorff and Pearson, 1999; Griffiths et al., 2017; Villnäs and Norkko, 2011) and other (sub)polar areas (Lalumière et al., 1994; Mattila et al., 1999) which may make them more sensitive to species loss than richer lower latitude seagrass ecosystems due to lower functional redundancy (Bonsdorff and Pearson, 1999; Griffiths et al., 2017).

Although the macrobenthic community structure was not significantly influenced by our levels of fertilisation their bioturbation activity was, suggesting that our levels of nutrient enrichment cued changes in the behaviour of apparent tolerant macro infauna. Indeed, mixing depth (MPD) and sediment reworking rate ($D_b$) decreased with increasing fertilisation, suggesting that macroinfauna burrowed shallower in these treatments (Figure

643 3B). There are two mechanisms to explain this result. First, porewater reduced chemical
644 species concentrations (in deep layers of the sediment) may have increased above the
645 tolerance level of these species (mainly *M. arenaria* and *H. diversicolor*) limiting their
646 suitable habitat to the first cm of the sediment column. Indeed, similarly to seagrasses,
647 reduced chemical species can be toxic for macroinfauna in high concentrations (Kristensen
648 and Kostka, 2005). Second, the increase of OM content at the sediment surface may have
649 met the feeding needs of the macrobenthic community, which did not need to forage deep
650 within the sediment column (Miller et al., 1996).

651 Contrary to the reduction of sediment reworking, the porewater exchange rates
652 increased with fertilisation intensity (Figure 3A). Porewater exchange rate largely depends
653 on (1) the surface of the sediment-water interface, which increases with burrow length, and
654 (2) ventilation activity of macrofauna, which enhance both advective porewater and
655 diffusive solute transports (Kristensen et al., 2012). Given that burrowing depth decreased
656 with nutrient enrichment, as suggested by lower MPD, it is most likely that macroinfauna
657 have increased their ventilation activity. There was no evidence of decreasing oxygen
658 concentration in the overlying water in enriched treatment (see appendix A). However,
659 several studies have shown that ventilation activity is triggered by a minimum threshold
660 value of oxygen concentration (*e.g.*, Pascal et al., 2019; Timmermann et al., 2006). The
661 increase of oxygen consumption in enriched treatments (Figure 4B and Figure 6) probably
662 triggered the onset of ventilation activity more frequently as compared to the control.

663 **4.5 Changes in benthic fluxes**

664 The increase of TOU in enriched treatments was an order of magnitude higher than
665 the one of DOU (Figure 6) indicating that other processes than OM mineralisation and

reoxidation of reduced chemical species by $O_2$ contributed to TOU. This result is in good agreement with the higher porewater exchange rate (as proxy of sediment bioirrigation) in enriched treatments. The increase of SOM at the sediment surface may also have enhanced metabolism of the macrobenthic community (Brockington and Clarke, 2001). During both May and August experiments, the increase of TOU tended to be triggered by a lower level of fertilisation in unvegetated than in vegetated areas, suggesting, here again, that unvegetated areas were more sensitive to fertilisation than vegetated areas.

$NO_x$ and $NH_4^+$ tightly interact within nitrogen cycling and will thus be discussed simultaneously. $NO_x$ and $NH_4^+$ benthic fluxes were barely detectable in the control suggesting that production (nitrification for $NO_x$ and organisms' excretion and microbial-mediated OM mineralization for $NH_4^+$) and consumption processes (nitrate reduction processes for $NO_x$ and primary produced uptake and nitrification for $NH_4^+$) offset each other. The increase in $NO_x$ and $NH_4^+$ benthic fluxes with fertilisation suggested that production processes overcame consumption ones. In May, this increase was totally explained by the increase of $NH_4^+$ and $NO_x$ diffusive fluxes with fertilisation, indicating that molecular diffusion was the major process controlling $NH_4^+$ and $NO_x$ fluxes at the sediment-water interface. On the contrary, the increase of $NH_4^+$ and $NO_x$ diffusive fluxes with fertilisation in August did not explain the totality of the increase of total $NH_4^+$ and $NO_x$ fluxes in enriched treatments, suggesting that other transport processes governed these fluxes at the sediment-water interface. The increase in total $NH_4^+$ and $NO_x$ fluxes may be attributed to the increase in macroinfauna ventilation activity and the resulting simulation of porewater exchange rate in enriched treatments. Together with the increase of porewater exchange rate, the decrease of MPD in enriched treatment may also explain the increase in

689 total $NO_x$ flux. Indeed, by reducing their burrowing depth were closer to the sediment layer
690 with higher $NO_x$ concentrations (nitrification zone *sensu* Michaud et al., 2006) and thus
691 enhanced nitrate efflux. Regarding $NH_4^+$, the increase of the total flux may also be
692 attributed to a higher metabolism of organisms (as hypothesised for TOU). Overall, these
693 results suggested that nutrient enrichment of the water column enhanced the release of
694 nutrient from the sediment to the overlying water (and thereby favoured its over
695 enrichment) through the increase of porewater nutrient concentration and the modification
696 of macroinfauna activity.

697 **5 Conclusion**

698 This experimental study demonstrated that changes in nutrient concentrations in the
699 water column not only affect the water column and the sediment surface but spread deeper
700 to the sediment column within a month timeframe with cascading effects on the sediment
701 biogeochemistry, the activity of benthic macrofauna and the whole ecosystem functioning.
702 The results presented here support the importance of seagrass meadows in the functioning
703 of coastal ecosystems. Indeed, our results confirm that within tolerance level (intermediate
704 level of fertilisation in the present study), the presence of seagrass buffers the effects of
705 fertilisation on SOM content and porewater reduced chemical species concentrations.
706 Managing the health of seagrass meadows could thus limit the eutrophication of coastal
707 water to some extent. The effects of fertilisation of the water column on benthic fluxes and
708 solute transport processes also depended on the seasonal timing of disturbance, which was
709 mainly related to differences in macrofauna densities (which were higher in summer than
710 in spring and higher in vegetated than unvegetated areas) and seagrass growing. Therefore,
711 environmental practitioners should consider this dynamic to undertake efficient

conservative measures. In addition, our results indicated that the fertilisation of the water column induced nutrient storage in porewater and nutrient fluxes from the sediment to the water column. This highlights that fertilisation can be self-sustaining in coastal waters and, thereby, can last even if conservative measures are taken to stop or reduce nutrient inputs from external sources of the ecosystem (*e.g.*, watershed). Finally, this study highlights the complex interconnected ecosystem processes involved in ecosystem functioning and their spatial and temporal variability in the context of nutrient enrichment.

**Acknowledgements**

We thank Frederik Belanger and Sylvain St-Onge from UQAR for their contribution to field work; Lisa Treau De Coeli and Laure de Montety from Université Laval for their assistance in macrofauna identification; Claude Belzile and Pascal Rioux (UQAR/ISMER) for their assistance in chemical analyses; Franck Gilbert (Université de Toulouse) for providing luminophores. We also thank the two reviewers for fruitful comments that greatly helped to improve the manuscript. LP is grateful to Sophie Moisset for her stimulating discussion and support. This study is a contribution to the research program of Québec-Océan.

**Funding**

This work is financially supported by the "RESILIENCE COTIERE" project funded to PB by "Fonds vert dans le cadre du Plan d'action sur les changements climatiques 2013–2020 (PACC 2013–2020) du gouvernement du Québec" and the "Expertise collective sur l'eutrophisation et la qualité des eaux côtières : vers l'appropriation des connaissances" project funded to GC by the "programme Odyssée Saint Laurent" from the "Réseau Québec Maritime". This research is also sponsored by the NSERC Canadian

735 Healthy Oceans Network and its Partners: Department of Fisheries and Oceans Canada and
736 INREST (representing the Port and the city of Sept-Îles) **[grant number 468437]**. LP was
737 supported by a postdoctoral fellowship B3X **[grant number 281864]** from FRQNT
738 (Quebec Funds for Research in Nature and Technology) and a postdoctoral fellowship
739 **[grant number PDF-25-2020]** from NCE-MEOPAR (Network of Center of Excellence -
740 Marine Environmental Observation, Prediction and Response).

741 **CRediT author statement**

742 **Ludovic Pascal**: Conceptualization, Methodology, Validation, Formal analysis,
743 Investigation, Writing – Original draft, Writing – Review & Editing, Visualization, Project
744 administration, Funding acquisition. **Gwénaëlle Chaillou:** Conceptualization,
745 Methodology, Validation, Resources, Writing – Review & Editing, Supervision, Project
746 administration, Funding acquisition. **Christian Nozais:** Resources, Writing – Review &
747 Editing. **Joannie Cool:** Investigation. **Pascal Bernatchez:** Resources, Writing – Review
748 & Editing, Supervision, Project administration, Funding acquisition. **Kevin Letourneux:**
749 Investigation. **Philippe Archambault:** Conceptualization, Methodology, Validation,
750 Resources, Writing – Review & Editing, Supervision, Project administration, Funding
751 acquisition.

752 **Conflicts of interest**

753 The authors declare no conflict of interest. The funding sponsors had no role in the
754 design of the study; in the collection, analyses, or interpretation of data; in the writing of
755 the manuscript, and in the decision to publish the results

The published version can be found at: https://doi.org/10.1016/j.marenvres.2022.105584

## Data availability statement

The data supporting the results are available on Scholar Portal Dataverse at https://doi.org/10.5683/sp3/aofpuz (Pascal et al., 2022)

## References

Alcoverro, T., Romero, J., Duarte, C.M., López, N.I., 1997. Spatial and temporal variations in nutrient limitation of seagrass *Posidonia oceanica* growth in the NW Mediterranean. Mar. Ecol. Prog. Ser. 146, 155–161. https://doi.org/10.3354/meps146155

Aller, R.C., Aller, J.Y., 1998. The effect of biogenic irrigation intensity and solute exchange on diagenetic reaction rates in marine sediments. J. Mar. Res. 56, 905–936.

Anschutz, P., Chaillou, G., Lecroart, P., 2007. Phosphorus diagenesis in sediment of the Thau Lagoon. Estuar. Coast. Shelf Sci. 72, 447–456. https://doi.org/10.1016/j.ecss.2006.11.012

Asmala, E., Gustafsson, C., Krause-Jensen, D., Norkko, A., Reader, H., Staehr, P.A., Carstensen, J., 2019. Role of Eelgrass in the Coastal Filter of Contrasting Baltic Sea Environments. Estuaries and Coasts 42, 1882–1895. https://doi.org/10.1007/s12237-019-00615-0

Barbier, E.B., Hacker, S.D., Kennedy, C.J., Koch, E.W., Stier, A.C., Silliman, B.R., 2011. The value of estuarine and coastal ecosystem services. Ecol. Monogr. 81, 169–193. https://doi.org/10.1890/10-1510.1

Bates, D., Machler, M., Bolker, B., Walker, S., 2015. Fitting Linear Mixed-Effects Models Using {lme4}. J. Stat. Softw. 67, 1–48. https://doi.org/10.18637/jss.v067.i01

Bonsdorff, E., Pearson, T.H., 1999. Variation in the sublittoral macrozoobenthos of the

779 Baltic Sea along environmental gradients: A functional-group approach. Austral Ecol.
780 24, 312–326. https://doi.org/10.1046/j.1442-9993.1999.00986.x
781 Borges, A., 2005. Do we have enough pieces of the jugsaw to integrate $CO_2$ fluxes in the
782 coastal ocean? Estuaries 28, 3–27.
783 Boström, C., Pittman, S., Simenstad, C., Kneib, R., 2011. Seascape ecology of coastal
784 biogenic habitats: advances, gaps, and challenges. Mar. Ecol. Prog. Ser. 427, 191–
785 217. https://doi.org/10.3354/meps09051
786 Brockington, S., Clarke, A., 2001. The relative influence of temperature and food on the
787 metabolism of a marine invertebrate. J. Exp. Mar. Bio. Ecol. 258, 87–99.
788 https://doi.org/10.1016/S0022-0981(00)00347-6
789 Brodersen, K.E., Hammer, K.J., Schrameyer, V., Floytrup, A., Rasheed, M.A., Ralph, P.J.,
790 Kühl, M., Pedersen, O., 2017. Sediment resuspension and deposition on seagrass
791 leaves impedes internal plant aeration and promotes phytotoxic $H_2S$ intrusion. Front.
792 Plant Sci. 8. https://doi.org/10.3389/fpls.2017.00657
793 Brodersen, K.E., Lichtenberg, M., Paz, L.C., Kühl, M., 2015. Epiphyte-cover on seagrass
794 (*Zostera marina* L.) leaves impedes plant performance and radial $O_2$ loss from the
795 below-ground tissue. Front. Mar. Sci. 2, 1–11.
796 https://doi.org/10.3389/fmars.2015.00058
797 Brun, F.G., Hernández, I., Vergara, J.J., Peralta, G., Pérez-Lloréns, J.L., 2002. Assessing
798 the toxicity of ammonium pulses to the survival and growth of *Zostera noltii*. Mar.
799 Ecol. Prog. Ser. 225, 177–187. https://doi.org/10.3354/meps225177
800 Burkholder, J., Mason, K., Glasgow, H., 1992. Water-column nitrate enrichment promotes
801 decline of eelgrass *Zostera marina*: evidence from seasonal mesocosm experiments.

802 Mar. Ecol. Prog. Ser. 81, 163–178. https://doi.org/10.3354/meps081163
803 Burkholder, J.M., Tomasko, D.A., Touchette, B.W., 2007. Seagrasses and eutrophication.
804 J. Exp. Mar. Bio. Ecol. 350, 46–72. https://doi.org/10.1016/j.jembe.2007.06.024
805 Chauvaud, L., Jean, F., Ragueneau, O., Thouzeau, G., 2000. Long term variation of the
806 Bay of Brest ecosystem : benthic pelagic-coupling revisited. Mar. Ecol. Prog. Ser.
807 200, 35–48. https://doi.org/10.3354/meps200035
808 Cochran, J.K., 1985. Particle mixing rates in sediments of the eastern equatorial Pacific:
809 Evidence from $^{210}$Pb, $^{239}$,$^{240}$Pu and $^{137}$Cs distributions at MANOP sites. Geochim.
810 Cosmochim. Acta 49, 1195–1210. https://doi.org/10.1016/0016-7037(85)90010-9
811 Coverly, S., Aminot, A., Kérouel, R., 2009. Nutrients in Seawater Using Segmented Flow
812 Analysis, in: Practical Guidelines for the Analysis of Seawater. CRC Press.
813 https://doi.org/10.1201/9781420073072.ch8
814 Deflandre, B., Duchêne, J.-C., 2010. PRO2FLUX – A software program for profile
815 quantification and diffusive $O_2$ flux calculations. Environ. Model. Softw. 25, 1059–
816 1061. https://doi.org/10.1016/J.ENVSOFT.2009.10.015
817 Diaz, R.J., Rosenberg, R., 2008. Spreading dead zones and consequences for marine
818 ecosystems. Science 321, 926–929.
819 Dunic, J.C., Brown, C.J., Connolly, R.M., Turschwell, M.P., Côté, I.M., 2021. Long-term
820 declines and recovery of meadow area across the world's seagrass bioregions. Glob.
821 Chang. Biol. gcb.15684. https://doi.org/10.1111/gcb.15684
822 Gattuso, J.-P., Frankignoulle., M., Wollast, R., 1998. Carbon and Carbonate Metabolism
823 in Coastal Aquatic Ecosystems. Annu. Rev. Ecol. Syst. 29, 405–434.
824 https://doi.org/10.1146/annurev.ecolsys.29.1.405

825 Glud, R.N., 2008. Oxygen dynamics of marine sediments. Mar. Biol. Res. 4, 243–289.
826 https://doi.org/10.1080/17451000801888726
827 Grall, J., Chauvaud, L., 2002. Marine eutrophication and benthos: The need for new
828 approaches and concepts. Glob. Chang. Biol. 8, 813–830.
829 https://doi.org/10.1046/j.1365-2486.2002.00519.x
830 Grasshoff, K., Ehrhardt, M., Kremling, K., 1999. Methods of Seawater Analysis, Wiley-
831 Vch. ed.
832 Griffiths, J.R., Kadin, M., Nascimento, F.J.A., Tamelander, T., Törnroos, A., Bonaglia, S.,
833 Bonsdorff, E., Brüchert, V., Gårdmark, A., Järnström, M., Kotta, J., Lindegren, M.,
834 Nordström, M.C., Norkko, A., Olsson, J., Weigel, B., Žydelis, R., Blenckner, T.,
835 Niiranen, S., Winder, M., 2017. The importance of benthic–pelagic coupling for
836 marine ecosystem functioning in a changing world. Glob. Chang. Biol. 23, 2179–
837 2196. https://doi.org/10.1111/gcb.13642
838 Hemminga, M.A., Duarte, C.M., 2000. Seagrass ecology. Cambridge University Press.
839 Hochard, S., Royer, F., Hubert, M., Lemonnier, H., 2019. Temporal variability of benthic-
840 pelagic coupling in shallow enclosed environment: A case study with eutrophying
841 shrimp ponds. Mar. Environ. Res. 146, 46–56.
842 https://doi.org/10.1016/j.marenvres.2019.03.005
843 Hope, J.A., Paterson, D.M., Thrush, S.F., 2020. The role of microphytobenthos in soft-
844 sediment ecological networks and their contribution to the delivery of multiple
845 ecosystem services. J. Ecol. 108, 815–830. https://doi.org/10.1111/1365-2745.13322
846 Joubert, J.-E., Bachand, E., 2012. Un marais en changement, caractérisation du marais salé
847 de la baie de Kamouraska. Com. ZIP du Sud-de-l'Estuaire, Rimouski, Québec, 123 p.

848 Kristensen, E., Kostka, J., 2005. Macrofaunal burrows and irrigation in marine sediment:
849 microbiological and biogeochemical interactions, in: Macro- and Microorganisms in
850 Marine Sediments. pp. 125–157. https://doi.org/10.1029/60CE08
851 Kristensen, E., Penha-Lopes, G., Delefosse, M., Valdemarsen, T., Quintana, C., Banta, G.,
852 2012. What is bioturbation? The need for a precise definition for fauna in aquatic
853 sciences. Mar. Ecol. Prog. Ser. 446, 285–302. https://doi.org/10.3354/meps09506
854 Lalumière, R., Messier, D., Fournier, J.-J., Peter McRoy, C., 1994. Eelgrass meadows in a
855 low arctic environment, the northeast coast of James Bay, Québec. Aquat. Bot. 47,
856 303–315. https://doi.org/10.1016/0304-3770(94)90060-4
857 Lapointe, B.E., Herren, L.W., Brewton, R.A., Alderman, P.K., 2020. Nutrient over-
858 enrichment and light limitation of seagrass communities in the Indian River Lagoon,
859 an urbanized subtropical estuary. Sci. Total Environ. 699, 134068.
860 https://doi.org/10.1016/j.scitotenv.2019.134068
861 Lee, K.-S., Park, S.R., Kim, Y.K., 2007. Effects of irradiance, temperature, and nutrients
862 on growth dynamics of seagrasses: A review. J. Exp. Mar. Bio. Ecol. 350, 144–175.
863 https://doi.org/10.1016/j.jembe.2007.06.016
864 Lepore, B.J., Barak, P., 2009. A Colorimetric Microwell Method for Determining Bromide
865 Concentrations. Soil Sci. Soc. Am. J. 73, 1130.
866 https://doi.org/10.2136/sssaj2007.0226
867 Link, H., Chaillou, G., Forest, A., Piepenburg, D., Archambault, P., 2013. Multivariate
868 benthic ecosystem functioning in the Arctic-benthic fluxes explained by
869 environmental parameters in the southeastern Beaufort Sea. Biogeosciences 10,
870 5911–5929. https://doi.org/10.5194/bg-10-5911-2013

871 Lohrer, A.M., Thrush, S.F., Gibbs, M.M., 2004. Bioturbators enhance ecosystem function
872 through complex biogeochemical interactions. Nature 431, 1092–1095.
873 https://doi.org/10.1038/nature03042
874 Marbà, N., Holmer, M., Gacia, E., Barron, C., 2007. Seagrass Beds and Coastal
875 Biogeochemistry, in: SEAGRASSES: BIOLOGY, ECOLOGYAND
876 CONSERVATION. Springer Netherlands, Dordrecht, pp. 135–157.
877 https://doi.org/10.1007/978-1-4020-2983-7_6
878 Mattila, J., Chaplin, G., Eilers, M.R., Heck, K.L., O'Neal, J.P., Valentine, J.F., 1999.
879 Spatial and diurnal distribution of invertebrate and fish fauna of a Zostera marina bed
880 and nearby unvegetated sediments in Damariscotta River, Maine (USA). J. Sea Res.
881 41, 321–332. https://doi.org/10.1016/S1385-1101(99)00006-4
882 Michaud, E., Desrosiers, G., Mermillod-Blondin, F., Sundby, B., Stora, G., 2006. The
883 functional group approach to bioturbation: II. The effects of the *Macoma balthica*
884 community on fluxes of nutrients and dissolved organic carbon across the sediment–
885 water interface. J. Exp. Mar. Bio. Ecol. 337, 178–189.
886 https://doi.org/10.1016/j.jembe.2006.06.025
887 Middelburg, J.J., 2019. Marine Carbon Biogeochemistry: A Primer for Earth System
888 Scientists, Springer Briefs in Earth System Sciences. https://doi.org/10.1007/978-3-
889 030-10822-9
890 Miller, D.C., Geider, R.J., Macintyre, H.L., 1996. Microphytobenthos: The ecological role
891 of the "secret garden" of unvegetated, shallow-water marine habitats. II. Role in
892 sediment stability and shallow-water food webs. Estuaries 19, 202–212.
893 https://doi.org/10.2307/1352225

894 Moreno-Marín, F., Vergara, J.J., Pérez-Llorens, J.L., Pedersen, M.F., Brun, F.G., 2016.
895 Interaction between ammonium toxicity and green tide development over seagrass
896 meadows: A laboratory study. PLoS One 11.
897 https://doi.org/10.1371/journal.pone.0152971
898 Nielsen, L.P., 1992. Denitrification in sediment determined from nitrogen isotope pairing.
899 FEMS Microbiol. Ecol. 86, 357–362.
900 Nixon, S.W., 1998. Enriching the sea to death. Sci. Am. Present. 48–53.
901 Noisette, F., Depetris, A., Kühl, M., Brodersen, K.E., 2020. Flow and epiphyte growth
902 effects on the thermal, optical and chemical microenvironment in the leaf
903 phyllosphere of seagrass (*Zostera marina*). J. R. Soc. Interface 17, 20200485.
904 https://doi.org/10.1098/rsif.2020.0485
905 Oksanen, J., Blanchet, F.G., Friendly, M., Kindt, R., Legendre, P., McGlinn, D., Minchin,
906 P.R., O'Hara, R.B., Simpson, G.L., Solymos, P., Stevens, M.H.H., Szoecs, E., Helene,
907 W., 2019. vegan: community Evology Package. R package version 2.5-5.
908 Orth, R.J., Carruthers, T.J.B., Dennison, W.C., Duarte, C.M., Fourqurean, J.W., Heck,
909 K.L., Hughes, A.R., Kendrick, G.A., Kenworthy, W.J., Olyarnik, S., Short, F.T.,
910 Waycott, M., Williams, S.L., 2006. A global crisis for seagrass ecosystems.
911 Bioscience 56, 987–996. https://doi.org/10.1641/0006-
912 3568(2006)56[987:AGCFSE]2.0.CO;2
913 Pascal, L., Bernatchez, P., Chaillou, G., Nozais, C., Lapointe Saint-Pierre, M.,
914 Archambault, P., 2020. Sea ice increases benthic community heterogeneity in a
915 seagrass landscape. Estuar. Coast. Shelf Sci. 243, 106898.
916 https://doi.org/10.1016/j.ecss.2020.106898

Pascal, L., Chaillou, G., Nozais, C., Cool, J., Bernatchez, P., Archambault, P., 2022. Data from: Benthos response to nutrient enrichment and functional consequences in coastal ecosystems. https://doi.org/10.5683/SP3/AOFPUZ

Pascal, L., Maire, O., Deflandre, B., Romero-Ramirez, A., Grémare, A., 2019. Linking behaviours, sediment reworking, bioirrigation and oxygen dynamics in a soft-bottom ecosystem engineer: The mud shrimp *Upogebia pusilla* (Petagna 1792). J. Exp. Mar. Bio. Ecol. 516, 67–78. https://doi.org/10.1016/j.jembe.2019.05.007

Pearson, T.H., Rosenberg, R., 1978. Macrobenthic succession in relation to organic enrichment and pollution of the marine environment. Oceanogr. Mar. Biol. Annu. Rev. 16, 229–311.

R Core Team, 2020. R: A Language and Environment for Statistical Computing.

Rabalais, N.N., Turner, R.E., Díaz, R.J., Justić, D., 2009. Global change and eutrophication of coastal waters. ICES J. Mar. Sci. 66, 1528–1537. https://doi.org/10.1093/icesjms/fsp047

Rao, A.M.F., Malkin, S.Y., Montserrat, F., Meysman, F.J.R., 2014. Alkalinity production in intertidal sands intensified by lugworm bioirrigation. Estuar. Coast. Shelf Sci. 148, 36–47. https://doi.org/10.1016/j.ecss.2014.06.006

Riaux-Gobin, C., Klein, B., 1993. Microphytobenthic Biomass Measurement using HPLC and conventional Pigment Analysis. Handb. methods using HPLC Conv. Pigment Anal. 369–376.

Riedel, B., Diaz, R., Rosenberg, R., Stachowitsch, M., 2016. The ecological consequences of marine hypoxia: from behavioural to ecosystem responses, in: Solan, M., Whiteley, N.M. (Eds.), Stressors in the Marine Environment. Oxford University Press, pp. 175–

194. https://doi.org/10.1093/acprof

Slomp, C.P., 2012. Phosphorus Cycling in the Estuarine and Coastal Zones: Sources, Sinks, and Transformations, Treatise on Estuarine and Coastal Science. Elsevier Inc. https://doi.org/10.1016/B978-0-12-374711-2.00506-4

Snelgrove, P.V.R., Soetaert, K., Solan, M., Thrush, S., Wei, C.-L., Danovaro, R., Fulweiler, R.W., Kitazato, H., Ingole, B., Norkko, A., Parkes, R.J., Volkenborn, N., 2018. Global Carbon Cycling on a Heterogeneous Seafloor. Trends Ecol. Evol. 33, 96–105. https://doi.org/10.1016/j.tree.2017.11.004

Soetaert, K., Petzoldt, T., 2020. marelac: Tools for Aquatic Sciences.

Soetaert, K., Petzoldt, T., 2010. Inverse modelling, sensitivity and monte carlo analysis in R using package FME. J. Stat. Softw. 33, 1–28. https://doi.org/10.18637/jss.v033.i03

Song, G.D., Liu, S.M., Marchant, H., Kuypers, M.M.M., Lavik, G., 2013. Anammox, denitrification and dissimilatory nitrate reduction to ammonium in the East China Sea sediment. Biogeosciences 10, 6851–6864. https://doi.org/10.5194/bg-10-6851-2013

Stockdale, A., Davison, W., Zhang, H., 2009. Micro-scale biogeochemical heterogeneity in sediments: A review of available technology and observed evidence. Earth-Science Rev. 92, 81–97. https://doi.org/10.1016/j.earscirev.2008.11.003

Timmermann, K., Banta, G.T., Glud, R.N., 2006. Linking *Arenicola marina* irrigation behavior to oxygen transport and dynamics in sandy sediments. J. Mar. Res. 64, 915–938. https://doi.org/10.1357/002224006779698378

Touchette, B.W., Burkholder, J.M., 2000. Review of nitrogen and phosphorus metabolism in seagrasses. J. Exp. Mar. Bio. Ecol. 250, 133–167. https://doi.org/10.1016/S0022-0981(00)00195-7

963 Van Der Heide, T., Smolders, A.J.P., Rijkens, B.G.A., Van Nes, E.H., Van Katwijk, M.M.,
964 Roelofs, J.G.M., 2008. Toxicity of reduced nitrogen in eelgrass (*Zostera marina*) is
965 highly dependent on shoot density and pH. Oecologia 158, 411–419.
966 https://doi.org/10.1007/s00442-008-1155-2
967 Veuger, B., van Oevelen, D., 2011. Long-term pigment dynamics and diatom survival in
968 dark sediment. Limnol. Oceanogr. 56, 1065–1074.
969 https://doi.org/10.4319/lo.2011.56.3.1065
970 Villnäs, A., Norkko, A., 2011. Benthic diversity gradients and shifting baselines:
971 Implications for assessing environmental status. Ecol. Appl. 21, 2172–2186.
972 https://doi.org/10.1890/10-1473.1
973 Volkenborn, N., Woodin, S.A., Wethey, D.S., Polerecky, L., 2016. Bioirrigation in Marine
974 Sediments, Reference Module in Earth Systems and Environmental Sciences.
975 https://doi.org/10.1016/B978-0-12-409548-9.09525-7
976 Waycott, M., Duarte, C.M., Carruthers, T.J.B., Orth, R.J., Dennison, W.C., Olyarnik, S.,
977 Calladine, A., Fourqurean, J.W., Heck, K.L., Hughes, A.R., Kendrick, G.A.,
978 Kenworthy, W.J., Short, F.T., Williams, S.L., 2009. Accelerating loss of seagrasses
979 across the globe threatens coastal ecosystems. Proc. Natl. Acad. Sci. U. S. A. 106,
980 12377–12381. https://doi.org/10.1073/pnas.0905620106
981 Wickham, H., 2016. ggplot2: Elegant Graphics for Data Analysis. Springer-Verlag, New
982 York.
983 Wollast, R., 1998. Evaluation and comparison of the global carbon cycle in the coastal
984 zone and in the open ocean, in: Brink, K.H., Robinson, A.R. (Eds.), The Sea. John
985 Wiley & Sons, Ltd, pp. 213–252.

The published version can be found at: https://doi.org/10.1016/j.marenvres.2022.105584

986

The published version can be found at: https://doi.org/10.1016/j.marenvres.2022.105584

# Appendix

## A. Realized fertilisation

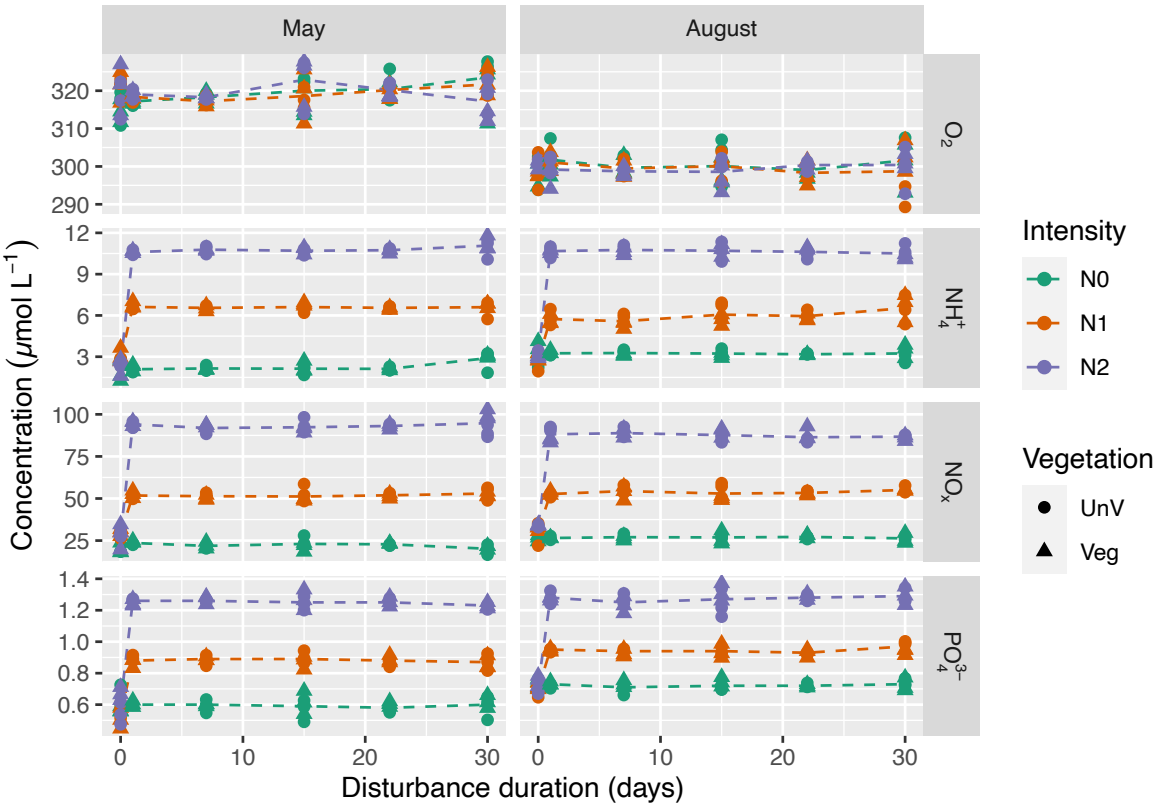


Fig. A.1: $O_2$, $NH_4^+$, $NO_x$ and $PO_4^{3-}$ concentration in the overlying water of experimental enclosure over the course of experiment duration.

The published version can be found at: https://doi.org/10.1016/j.marenvres.2022.105584

## B. Statistical results

Table B. 1: ANOVA results of factors effects on sediment organic matter (SOM), chlorophyll *a* (Chl $_a$) and phaeopigments (Phaeo).
Significance codes: p < 0.05 = *, p < 0.01 = **, p < 0.001 = ***
Source of variation codes: V = Vegetation, I = Fertilisation intensity, M = Month

| Variable | Source of variation | SS | df | F | p | Significance |
|---|---|---|---|---|---|---|
| SOM | V | 3.618 | 1 | 40.609 | < 0.001 | *** |
| | I | 36.302 | 2 | 203.713 | < 0.001 | *** |
| | M | 19.703 | 1 | 221.127 | < 0.001 | *** |
| | V x I | 3.615 | 2 | 20.288 | < 0.001 | *** |
| | V x M | 5.883 | 1 | 66.029 | < 0.001 | *** |
| | I x M | 1.385 | 2 | 7.775 | 0.002 | ** |
| | V x I x M | 0.795 | 2 | 4.462 | 0.023 | * |
| | Residuals | 2.138 | 24 | | | |
| Chl *a* | V | 2234.1 | 1 | 249.848 | < 0.001 | *** |
| | I | 3773.2 | 2 | 210.984 | < 0.001 | *** |
| | M | 236.6 | 1 | 26.459 | < 0.001 | *** |
| | V x I | 1375.7 | 2 | 76.925 | < 0.001 | *** |
| | V x M | 277.9 | 1 | 31.084 | < 0.001 | *** |
| | I x M | 197.0 | 2 | 11.015 | < 0.001 | *** |
| | V x I x M | 62.1 | 2 | 3.470 | 0.047 | * |
| | Residuals | 214.6 | 24 | | | |
| Phaeo | V | 180.45 | 1 | 114.173 | < 0.001 | *** |
| | I | 342.97 | 2 | 108.502 | < 0.001 | *** |
| | M | 1223.06 | 1 | 773.849 | < 0.001 | *** |
| | V x I | 77.29 | 2 | 24.451 | < 0.001 | *** |
| | V x M | 209.69 | 1 | 132.674 | < 0.001 | *** |
| | I x M | 200.85 | 2 | 63.539 | < 0.001 | *** |
| | V x I x M | 89.89 | 2 | 28.439 | < 0.001 | *** |
| | Residuals | 37.93 | 24 | | | |

The published version can be found at: https://doi.org/10.1016/j.marenvres.2022.105584

Table B. 2: ANOVA results of factors effects on seagrass leaf biomass and elongation.
Significance codes: p < 0.05 = *, p < 0.01 = **, p < 0.001 = ***
Source of variation codes: V = Vegetation, I = Fertilisation intensity, M = Month

| Variable | Source of variation | SS | df | F | p | Significance |
|---|---|---|---|---|---|---|
| Biomass | I | 0.127 | 2.000 | 11.180 | 0.002 | ** |
| | M | 13.563 | 1.000 | 2391.668 | < 0.001 | *** |
| | I x M | 0.018 | 2.000 | 1.605 | 0.241 | |
| | Residuals | 0.068 | 12.000 | | | |
| Elongation | I | 0.077 | 2.000 | 7.831 | 0.007 | ** |
| | M | 0.136 | 1.000 | 27.619 | < 0.001 | *** |
| | I x M | 0.091 | 2.000 | 9.218 | 0.004 | ** |
| | Residuals | 0.059 | 12.000 | | | |

The published version can be found at: https://doi.org/10.1016/j.marenvres.2022.105584

Table B. 3: PERMANOVA results of factors effects on macrofauna community structure. Bold indicates the source of variation depicted in the corresponding figure.
Significance codes: p < 0.05 = *, p < 0.01 = **, p < 0.001 = ***
Source of variation codes: V = Vegetation, I = Fertilisation intensity, M = Month

| Source of variation | SS | df | F | p | Significance |
|---|---|---|---|---|---|
| V | 1.042 | 1 | 14.755 | < 0.001 | *** |
| I | 0.011 | 2 | 0.075 | 1.000 | |
| M | 3.497 | 1 | 49.539 | < 0.001 | *** |
| V x I | 0.020 | 2 | 0.138 | 0.967 | |
| **V x M** | **1.019** | **1** | **14.427** | **< 0.001** | *** |
| I x M | 0.012 | 2 | 0.084 | 0.977 | |
| V x I x M | 0.011 | 2 | 0.076 | 0.998 | |
| Residuals | 1.694 | 24 | | | |

The published version can be found at: https://doi.org/10.1016/j.marenvres.2022.105584

Table B. 4: ANOVA results of factors effects on bioturbation metrics (Q: porewater exchange rate; MPD: maximum penetration depth of luminophore; $D_b$: biodiffusion coefficient). Bold indicates the source of variation depicted in the corresponding figure.
Significance codes: p < 0.05 = *, p < 0.01 = **, p < 0.001 = ***
Source of variation codes: V = Vegetation, I = Fertilisation intensity, M = Month

| Variable | Source of variation | SS | df | F | p | Significance |
|---|---|---|---|---|---|---|
| Q | V | 0.035 | 1 | 0.081 | 0.778 | |
| | I | 28.210 | 2 | 32.738 | < 0.001 | *** |
| | M | 27.834 | 1 | 64.606 | < 0.001 | *** |
| | **V x I** | **3.563** | **2** | **4.135** | **0.029** | * |
| | V x M | 2.167 | 1 | 5.031 | 0.034 | * |
| | I x M | 9.518 | 2 | 11.046 | < 0.001 | *** |
| | V x I x M | 0.391 | 2 | 0.454 | 0.640 | |
| | Residuals | 10.73 | 24 | | | |
| MPD | V | 0.043 | 1 | 0.132 | 0.719 | |
| | I | 95.462 | 2 | 145.466 | < 0.001 | *** |
| | M | 0.016 | 1 | 0.048 | 0.829 | |
| | **V x I** | **3.962** | **2** | **6.037** | **0.008** | ** |
| | V x M | 1.266 | 1 | 3.857 | 0.061 | |
| | I x M | 8.073 | 2 | 12.302 | < 0.001 | *** |
| | V x I x M | 1.573 | 2 | 2.397 | 0.112 | |
| | Residuals | 7.875 | 24 | | | |
| $D_b$ | V | 113.420 | 1 | 59.315 | < 0.001 | *** |
| | I | 468.770 | 2 | 122.577 | < 0.001 | *** |
| | M | 2.590 | 1 | 1.353 | 0.256 | |
| | **V x I** | **56.010** | **2** | **14.646** | **< 0.001** | *** |
| | V x M | 4.040 | 1 | 2.110 | 0.159 | |
| | I x M | 4.510 | 2 | 1.180 | 0.324 | |
| | V x I x M | 10.460 | 2 | 2.736 | 0.085 | |
| | Residuals | 45.890 | 24 | | | |

The published version can be found at: https://doi.org/10.1016/j.marenvres.2022.105584

Table B. 5: ANOVA results of factors effects on oxygen penetration depth (OPD) and diffusive oxygen uptake (DOU). Bold indicates the source of variation depicted in the corresponding figure.
Significance codes: p < 0.05 = *, p < 0.01 = **, p < 0.001 = ***
Source of variation codes: V = Vegetation, I = Fertilisation intensity, M = Month, D = Fertilisation duration
[a]Box-Cox transformation, lambda = 0.5
[b]Box-Cox transformation, lambda = 0.8

| Variable | Source of variation | SS | df | F | p | Significance |
|---|---|---|---|---|---|---|
| OPD[a] | V | 386.41 | 1 | 12.6585 | < 0.001 | *** |
| | I | 1163.62 | 2 | 17.5449 | < 0.001 | *** |
| | D | 774.43 | 1 | 26.3507 | < 0.001 | *** |
| | M | 1447.07 | 1 | 41.7799 | < 0.001 | *** |
| | V x I | 103.07 | 2 | 1.5364 | 0.226 | |
| | V x D | 251.52 | 1 | 7.4212 | 0.009 | ** |
| | I x D | 1229.80 | 2 | 18.8118 | < 0.001 | *** |
| | V x M | 138.88 | 1 | 3.9424 | 0.053 | |
| | I x M | 152.38 | 2 | 2.1059 | 0.133 | |
| | D x M | 16.44 | 1 | 0.4274 | 0.517 | |
| | **V x I x D** | **427.25** | **2** | **6.0461** | **0.005** | ** |
| | V x I x M | 122.38 | 2 | 1.7671 | 0.182 | |
| | V x D x M | 0.99 | 1 | 0.0406 | 0.841 | |
| | I x D x M | 170.48 | 2 | 2.5231 | 0.091 | |
| | V x I x D x M | 69.62 | 2 | 1.0275 | 0.366 | |
| DOU[b] | V | 69.046 | 1 | 55.6814 | < 0.001 | *** |
| | I | 152.976 | 2 | 63.3374 | < 0.001 | *** |
| | D | 139.265 | 1 | 116.8962 | < 0.001 | *** |
| | M | 34.790 | 1 | 29.0847 | < 0.001 | *** |
| | V x I | 23.379 | 2 | 8.2582 | 0.001 | *** |
| | V x D | 19.628 | 1 | 15.4742 | < 0.001 | *** |
| | I x D | 117.453 | 2 | 49.9490 | < 0.001 | *** |
| | V x M | 3.786 | 1 | 3.0273 | 0.088 | |
| | I x M | 37.533 | 2 | 15.4986 | < 0.001 | *** |
| | D x M | 8.226 | 1 | 6.9588 | 0.011 | * |
| | V x I x D | 9.571 | 2 | 4.1340 | 0.022 | * |
| | V x I x M | 16.486 | 2 | 6.5040 | 0.003 | ** |
| | V x D x M | 3.935 | 1 | 3.0147 | 0.089 | |
| | I x D x M | 4.563 | 2 | 1.8052 | 0.176 | |
| | **V x I x D x M** | **10.223** | **2** | **4.0564** | **0.024** | * |

The published version can be found at: https://doi.org/10.1016/j.marenvres.2022.105584

Table B. 6: ANOVA results of factors effects on total oxygen uptake (TOU) and $NH_4^+$ and $NO_x$ total benthic fluxes. Bold indicates the source of variation depicted in the corresponding figure.
Significance (Sign) codes: p < 0.05 = *, p < 0.01 = **, p < 0.001 = ***
Source of variation codes: V = Vegetation, I = Fertilisation intensity, M = Month
[a]Box-Cox transformation, lambda = – 0.88

| | | TOU | | | | $NH_4^+$ [a] | | | | $NO_x$ | | | |
|---|---|---|---|---|---|---|---|---|---|---|---|---|---|
| **Source of variation** | **df** | **SS** | **F** | **p** | **Sign** | **SS** | **F** | **p** | **Sign** | **SS** | **F** | **p** | **Sign** |
| V | 1 | 17.946 | 110.682 | < 0.001 | *** | 0.001 | 0.37 | 0.552 | | 161.99 | 897.25 | < 0.001 | *** |
| I | 2 | 45.850 | 141.394 | < 0.001 | *** | 2.121 | 307.57 | < 0.001 | *** | 319.55 | 1769.93 | < 0.001 | *** |
| D | 1 | 77.846 | 480.127 | <0.001 | *** | 3.113 | 902.86 | < 0.001 | *** | 0.01 | 0.06 | 0.807 | |
| M | 1 | 16.787 | 103.536 | < 0.001 | *** | 0.517 | 149.98 | < 0.001 | *** | 136.74 | 378.70 | < 0.001 | *** |
| V x I | 2 | 4.351 | 13.417 | < 0.001 | *** | 0.043 | 6.36 | 0.013 | * | 148.41 | 822.04 | < 0.001 | *** |
| V x D | 1 | 2.526 | 15.581 | < 0.001 | *** | 0.012 | 3.62 | 0.065 | | 6.19 | 34.29 | < 0.001 | *** |
| I x D | 2 | 48.932 | 150.899 | <0.001 | *** | 1.920 | 278.55 | < 0.001 | *** | 0.33 | 1.80 | 0.188 | |
| V x M | 1 | 5.337 | 32.916 | < 0.001 | *** | 0.006 | 2.00 | 0.166 | | 224.92 | 622.90 | < 0.001 | *** |
| I x M | 2 | 0.162 | 0.499 | 0.611 | | 0.280 | 40.67 | < 0.001 | *** | 377.68 | 1045.97 | < 0.001 | *** |
| D x M | 1 | 0.547 | 3.374 | 0.075 | | 0.606 | 175.97 | < 0.001 | *** | 0.77 | 2.13 | 0.160 | |
| V x I x D | 2 | 4.299 | 13.256 | < 0.001 | *** | 0.009 | 1.37 | 0.267 | | 8.26 | 45.75 | < 0.001 | *** |
| V x I x M | 2 | 1.051 | 3.240 | 0.051 | | 0.027 | 4.02 | 0.027 | * | 240.04 | 664.77 | < 0.001 | *** |
| V x D x M | 1 | 2.454 | 15.138 | < 0.001 | *** | 0.040 | 11.73 | 0.002 | ** | 7.54 | 20.87 | < 0.001 | *** |
| I x D x M | 2 | 0.034 | 0.106 | 0.899 | | 0.379 | 55.01 | < 0.001 | *** | 2.24 | 6.21 | 0.005 | ** |
| **V x I x D x M** | **2** | **1.063** | **3.279** | **0.049** | * | **0.040** | **5.88** | **0.006** | ** | **4.55** | **12.59** | **< 0.001** | *** |

The published version can be found at: https://doi.org/10.1016/j.marenvres.2022.105584

1027